



Johannes Gross, BSc

**Enzymatic  
Stereoselective Dehalogenation of  
1,3-Dibromobutane**

**MASTERS'S THESIS**

To achieve the university degree of  
Diplom-Ingenieur  
Master's degree programme: Chemistry

Submitted to

**Graz University of Technology**

Supervisor

Prof. Dr. Kurt Faber

Dr. Melanie Hall

Department of Chemistry

University of Graz

Graz, May 2015

## **AFFIDAVIT**

I declare that I have authored this thesis independently, that I have not used other than the declared sources/resources, and that I have explicitly indicated all material which has been quoted either literally or by content from the sources used. The text document uploaded to TUGRAZonline is identical to the present master's thesis dissertation.

---

Date

---

Signature

*"Time is a drug.*

*Too much of it kills you"*

Terry Pratchett

# Acknowledgements

First of all, I want to thank my family, friends and especially the nufos for their very specific encouragement and support from childhood on, until now.

Special thanks and hugs to my love KTY – no words can express...

Thanks to the whole “Fab-Crew”. It has been a very impressive time. Special thanks to Wolfgang Kroutil for his support in many points (not only chemistry). Thanks to Verena Resch for all 3D-structures and Babsi for always being at the right place at the right time. I’d like to thank my supervisor Melanie Hall and Kurt Faber for all discussions, support and diverting stories. Also special thanks to Klaus Zangger and his working for group for the NMR-measurements.

I also thank Zbynek Prokop and his group from the University of Brno for all preliminary studies and the allocation of LinB.

# Zusammenfassung

Haloalkan-Dehalogenasen, wie LinB aus dem Organismus *Sphingomonas paucimobilis*, zählen zu den entgiftenden Enzymen, welche eine große Bandbreite an halogenierten Kohlenwasserstoffen als Substrate akzeptieren. Als Produkt der Hydrolyse des Halogenatoms entsteht der entsprechende Alkohol unter Inversion der Absolutkonfiguration. Basierend auf Vorversuchen der Universität Brno, wurden die Stereoselektivität und die Kinetik der Dehalogenierung von *rac*-1,3-Dibrombutan in Tris-Sulfat-Puffer bei pH 8.2 mit Hilfe der Dehalogenase LinB genauer untersucht. In Abhängigkeit von der Regioselektivität des Enzymes für das primäre bzw. sekundäre Halogenatom und der Präferenz des Enzyms für jeweils ein Enantiomer des racemischen Substrates wurden durch Substitution der Halogenatome die entsprechenden primären bzw. sekundären Mono-Alkohole gebildet, die in einem zweiten Reaktionsschritt zu den Diolen als Endprodukte umgesetzt wurden.

Ziel dieser Arbeit war die Bestimmung der Absolutkonfiguration der gebildeten regioisomeren Halo-Alkohole als Zwischenstufen und des Diol-Endproduktes, sowie die Enantiopräferenz für das Substrat.

Während das racemische Substrat und die Enantiomeren der Diol-Endprodukte kommerziell erhältlich waren, mussten Standards für die Enantiomere der Halo-Alkohol Intermediate chemisch synthetisiert werden. Mit Hilfe dieser unabhängig synthetisierten Referenzen konnten die GC-Peaks der Intermediate, sowie der Endprodukte eindeutig zugeordnet, und die Absolutkonfiguration bestimmt werden.

Somit konnte eindeutig bewiesen werden, dass das Enzym LinB das (*R*)-Enantiomer von *rac*-1,3-Dibrombutan bevorzugt, die Enantioselektivität der ersten Hydrolysestufe (ausgedrückt durch den E-Wert) liegt bei ca. 5. Das Enzym zeigt eine Regioselektivität für das sekundäre Halogenatom und bildet durch Inversion (*S*)-1-Brom-3-butanol mit einem E.e.<sub>max</sub> von 86%, das Regio-Isomer (*S*)-3-Brom-1-butanol entsteht langsamer mit einem E.e.<sub>max</sub> von >97%.

Die Reaktionsgeschwindigkeit im zweiten Hydrolyseschritt ist ebenfalls um den Faktor 5 bevorzugt, d.h. (*S*)-1-Brombutan-3-ol wird um den Faktor 5 schneller umgesetzt als (*S*)-3-Brom-1-butanol, wobei der zweite Reaktionsschritt eine niedrigere Enantioselektivität aufweist als der erste. Als Folge davon wird das Endprodukt (*S*)-1,3-Butandiol mit einem E.e.<sub>max</sub> von 35 % gebildet.

## Summary

Haloalkane dehalogenases, such as LinB from *Sphingomonas japonicum* (formerly *Sphingomonas paucimobilis*), are detoxifying enzymes which hydrolyze a wide range of halogenated compounds by replacing the halogen atom with a hydroxyl group with inversion of configuration. Following preliminary studies carried out at the University of Brno, Czech Republic, the dehalogenation of *rac*-1,3-dibromobutane was investigated using LinB in Tris-sulfate buffer at pH 8.2.

Depending on the regioselectivity of the enzyme (primary vs secondary halogen atom), and its enantioselectivity on the racemic substrate, the corresponding primary or secondary haloalcohol are formed, which are converted in a consecutive hydrolysis step to furnish 1,3-butanediol as end-product.

The goal of this thesis was to study and determine the enantio-preference of LinB on *rac*-1,3-dibromobutane and to determine the absolute configuration of the regioisomeric halo-alcohols formed as intermediates, as well as that of the diol end-product.

While *rac*-1,3-dibromobutane and both (*R*)- and (*S*)-1,3-butanediol were commercially available, standards for the enantiomers of the halo-alcohol-intermediates had to be independently synthesized. With the latter materials in hand, the absolute configuration of both intermediate products and the end-product could be unambiguously determined.

It could be proven that dehalogenase LinB exhibits pronounced regioselectivity for the secondary halogen atom in the first hydrolysis step and forms (*S*)-1-bromo-3-butanol through inversion of configuration with a  $E.e._{max}$  of 86%; the regioisomeric (*S*)-3-bromo-1-butanol is formed somewhat more slowly with a  $E.e._{max}$  of >97%. Thus, the enzyme prefers the (*R*)-enantiomer of *rac*-1,3-dibromobutane with poor enantioselectivity ( $E \sim 5$ ) in the hydrolysis occurring at the secondary halocarbon while the (*S*)-enantiomer is preferred in the hydrolysis taking place at the primary halocarbon. In the second step, a switch in regiopreference occurs as (*S*)-1-bromobutan-3-ol is converted five times faster than (*S*)-3-bromo-1-butanol. As a consequence, the end-product (*S*)-1,3-butanediol is formed with a  $E.e._{max}$  of 35 %.

# Table of contents

Acknowledgements .....	4
Zusammenfassung .....	5
Summary .....	6
Introduction .....	8
Haloalkanes Sources .....	8
Physical Properties.....	13
Halogenation .....	13
Dehalogenation .....	15
Haloalkane dehydrogenase LinB .....	22
Results and Discussion .....	25
General .....	26
Synthesis.....	27
Kinetic Resolution of 1,3-Dibromobutane .....	28
Experimental .....	30
General.....	30
Enzyme LinB .....	30
General Procedure for Biotransformation.....	31
Analytical Data .....	31
GC-FID Detector Calibration.....	32
Synthesis of Compounds.....	33
Biotransformation .....	38
Assignment of GC - Product Peaks .....	39
Kinetic Resolution of 1,3-Dibromobutane with LinB .....	42
Reaction Rate and Kinetic Coefficient k .....	43
Conclusions .....	48
References .....	49
Supplementary Data .....	50
Publications. ....	51

# 1 Introduction

## 1.1 Haloalkanes - Sources

On one hand, haloalkanes are chemically synthesized in industry on a large scale and on the other hand, haloalkanes are formed naturally too. There are also many substances which derive from both origins. Due to the significance of halo-organic compounds in organic chemistry and as solvents for technical processes, haloalkanes are omnipresent in daily life. [2]

### 1.1.1 Native sources

Actually, haloalkanes are not only synthetically produced by mankind, but are also assembled in nature by many different organisms. Up to date, more than 3500 halogen-metabolites have been identified. Some of them — like chloramphenicol or 7-chlorotetracyclin — are important antibiotics. [6]

In nature, haloalkanes are mostly formed by terrestrial organisms and in marine species and they encompass also surprisingly simple compounds, such as chloromethane, bromomethane and 1,2-dibromomethane. [2] [5]

Especially, low halogenated molecules were found among chloro- and bromo-alkanes. Higher halogenated analogs are bromoalkanes, like tribromomethane and bromomethane, of which up to  $10^7$  tons per year are released into the atmosphere by the coastal brown algae *Ascophyllum nodosum*. It is thought that haloalkanes are enzymatically produced in order to prevent the hosts from microbial attack. [5]

Due to the high amount of bromide in seawater, bromo-alkanes dominate in aquatic organisms, while chloro-alkanes are mostly synthesized by terrestrial organisms. Other (non-biological) mechanisms of formation are forest fires or geothermal and volcanic processes. The formation of fluoro-, chloro-, bromo- and iodo-haloalkanes in nature is reflected by the chemical properties of the halogen atom, which in turn determines its position in the periodic system. The biggest fraction of haloalkanes is made up by chloroalkanes, followed by bromo- and a small amount of iodoalkanes. Although fluorine is available in a rather high amount, there are just very few fluoroalkanes known, which reflects the difficulty in activation of fluorine. [1]

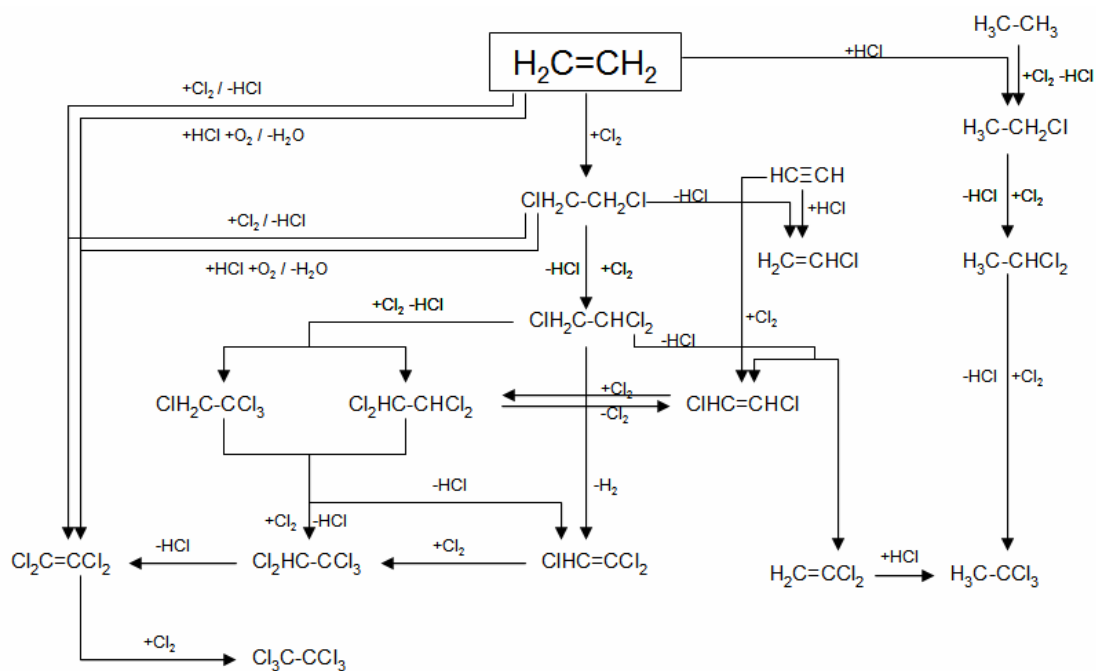
In many cases, halogenation processes in organisms are catalysed by haloperoxidases. That kind of enzyme use hydrogen peroxide for the oxidation of halide anions at the expense of hydrogen peroxide for the introduction of halogen into the substrate (see section 1.2).[3]

### **1.1.2 Anthropogenic sources**

The starting point of the introduction of a large amount of fluoro-chloro-hydrocarbons (FCCH) is congruent with the very beginnings of chloro-chemistry. Some properties are their high stability, hard flammability, high vapour pressure and their long lifetime. Once liberated in nature, FCCHs are disintegrated very slowly. These properties render FCCH's very interesting in many fields of chemistry. [2] To highlight the most important and hence most widely spread halo-organic compounds, they are used as:

- Solvents (e.g. dichloromethane, trichloromethane, trichloroethene)
- Metal degreasing (e.g. trichloroethane, tetrachloroethane)
- Starting materials of numerous chemical synthesis (e.g. chloro- and bromoalkanes)
- Cryogenic agents (e.g. dichlorodifluoromethane)

In addition to the above mentioned applications, organo-halogens are also ubiquitous in daily used agents like disinfectants, cleaning agents, pesticides, fungicides and flame-retardants. Important pathways for the synthesis of haloalkanes start from ethene as substrate and are shown in figure 1.[3]

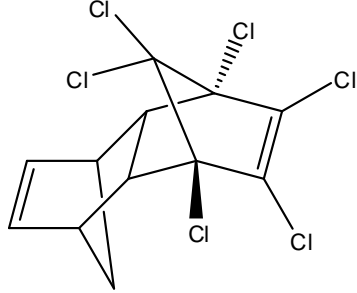
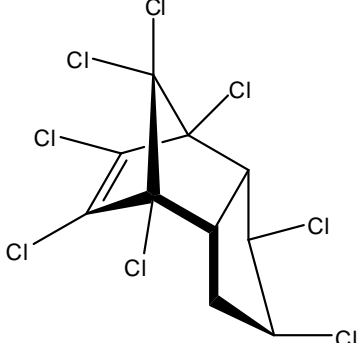
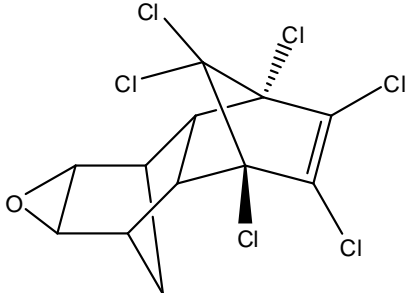
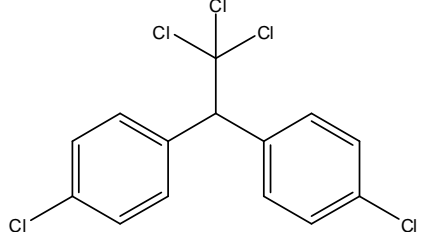
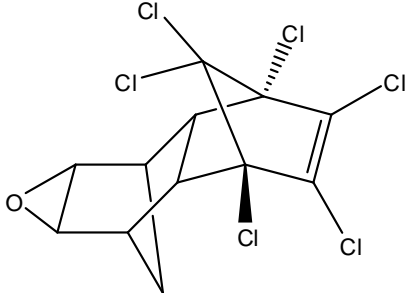


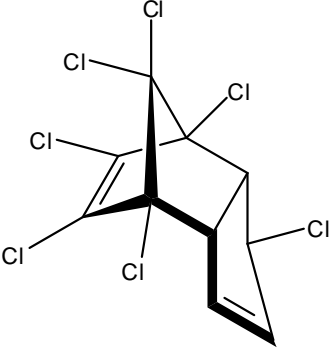
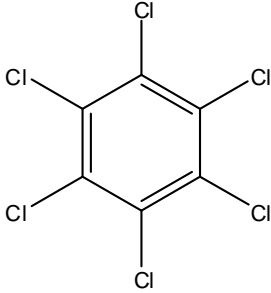
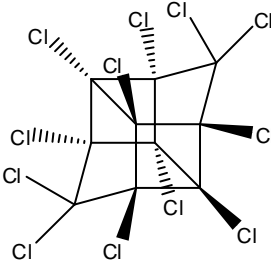
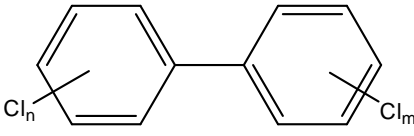
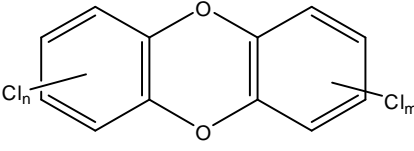
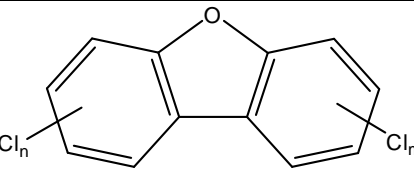
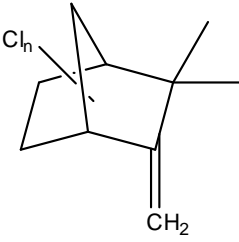
**Fig. 1** Systematic overview of halogenation starting with ethene [3]

In addition, many halogenated substances are produced unintentionally as side products (i.e. during incineration, e.g. dioxins or as minor products during chemical synthesis of halogenated organic compounds, such as pentachlorophenol, which is often used as intermediate in the agrochemical industry. In particular, many halo-aromatics are thought to be toxic and/or carcinogenic.[6]

In addition, the dirty dozen has to be mentioned (Table 1). These twelve persistent organic pollutions (POP) have been prohibited since 2001 by the POP-Convention (Stockholm Convention). The dirty dozen includes plant protecting agents, insecticides, industrial chemicals, and side products of burning processes.[17]

**Table 1:** List of the dirty dozen

	Aldrin
	Chlordane
	Dieldrin
	DDT
	Endrin

	Heptachlor
	HCB
	Mirex
	PCB
	Polychlorinated dibenzo dioxins
	Polychlorinated dibenzofurans
	Toxaphene

## 1.2 Physical properties

Compared to their chemical reactivity and physical properties, haloalkanes are quite different compared to the corresponding alkanes. Characteristics, like boiling points, bond lengths and -strengths are strongly depending on the halogen atom.

Due to the increasing size of the *p*-orbital from fluorine to iodine, the length of the C-X bond in haloalkanes increases. Due to the fact that the electronegativity of halogens is always higher than that of carbon, the C-X bond is polarised. Consequently, the electron density of the C-X bond is not symmetric, but shifted towards the halogen. The electrophilic  $\delta^+$  - carbon atom is now a good target for attack by electron-rich and nucleophilic groups. On the other hand, electron-deficient groups, like cations would be attacked by the  $\delta^-$  - halogen atom.

The polarity of the C-X bond shifts also the boiling point (BP), which is always higher than the BP of the corresponding alkanes. This is due to the formation of dipole-dipole interactions. Due to the increase of the atomic mass from fluorine to iodine, the BP's are increasing in the same direction within a homogeneous series of haloalkanes. [4]

## 1.3 Halogenation

Although just a few types of halogenating enzymes are known to date, the number of naturally formed haloalkanes is impressive. The major types of halogenating enzymes are:

- Flavin dependent halogenases
- $\alpha$ -Ketoglutarate dependent non-heme iron halogenases
- Haloperoxidases

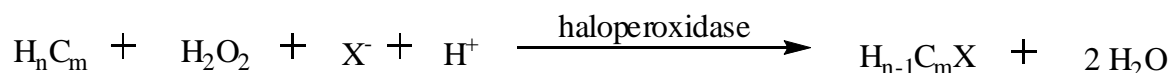


**Fig. 2** Schematic representation of enzymatic halogenation by haloperoxidases, with X being Cl, Br or I. [3] [5]

The major group of naturally formed halometabolites is formed by the redox enzyme haloperoxidase, which is widespread in nature. Haloperoxidases mediate the conversion of alkenes by a hypohalous acid (HOX), obtained via direct enzymatic oxidation of halide, yielding the halonium intermediate. [5] Once the reactive halogenating species is formed in the active site of the enzyme, it diffuses into the medium, where it performs a chemical (non-enzymatic) halogenation of a substrate. Consequently, halogenations mediated by haloperoxidases are usually not stereo-selective. The reaction pathways 1, 2 and 3 in figure 3 show the different product spectrum by using a hydroxy group (1), a carboxylic group (2) and a second halide ion (3) as nucleophile for the reaction with the initially formed halonium intermediate. Due to the large spectrum of structurally different haloalkanes and the small amount of different types of halogenating enzymes, the product selectivity of those enzymes is rather low.

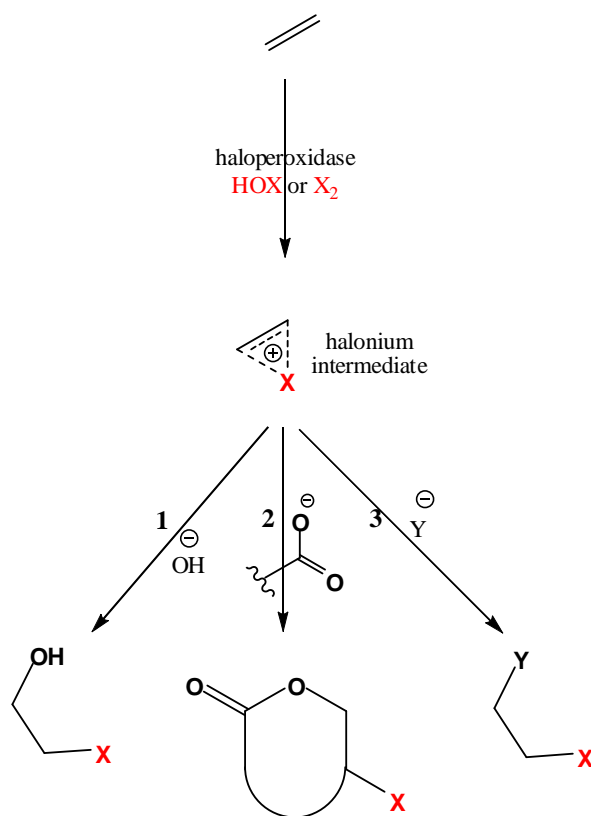


**Fig. 3** Transformation pathways of haloperoxidases starting with an alkene

## 1.4 Dehalogenation

Halogenated substances are a very important type of technical chemicals, of which a certain fraction is unavoidably released into the ecosphere. Owing to the fact, that halo-organic compounds are also produced by nature, a number of pathways have been evolved to ensure their microbial biodegradation. The isolation and characterisation of those organisms, which are involved in dehalogenation processes is important for the bioremediation of halo-organics. Without microbial dehalogenation, the amount of halogenated substances would rather fast pollute the ecosystem. There are just a few pathways for the degradation of haloalkanes. Those are given in table 2.

**Table 2** Pathways of enzymatic haloalkane degradation

Reaction type	Starting material	Products
Reductive dehalogenation	C-X	→ C-H + X <sup>-</sup>
Oxidative degradation	H-C-X	→ C=O + HX
Dehydrohalogenation	H-C-C-X	→ C=C + HX
Epoxide formation	HO-C-C-X	→ epoxide + HX
Hydrolysis	C-X + H <sub>2</sub> O	→ C-OH + HX

X = Cl, Br, I

(i) For the substitution of the halogen by a hydrogen atom, a redox system is applied, yielding the corresponding alkane.

(ii) Alternatively, oxidative degradation of halo-organics can occur.

(iii) In contrast, dehydrohalogenation is a redox-neutral process, where the elimination of hydrogen halide leads to the formation of the corresponding alkene intermediate, which is further degraded via oxidation.

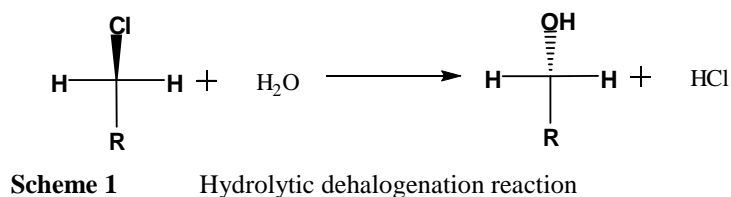
(iv) Dehydrohalogenation of a halohydrin is catalysed by haloalcohol dehalogenases, which yield the corresponding epoxide. The latter is hydrolytically further metabolised by epoxide hydrolases to furnish *vic*-diols.

(v) The nucleophilic substitution of the halide, which is typically responsible for the toxic properties, by e.g. a hydroxyl group to furnish the corresponding alcohol as innocuous degradation product going in hand with the release of halide anion, is the key step in enzymatic dehalogenation, which is catalysed by dehalogenases. [7] In the year 1960, a dehalogenase of bacterial origin was purified for the first time. This dehalogenase was involved in the dechlorination of 2-chloropropionic acid and chloroacetate, which are widely used chemicals. [6]

For pathways (i) - (iii), the interest for biocatalytic syntheses is small, because the corresponding transformations go in hand with the loss of the functional group or by destruction of a chiral centre.

In contrast, pathway (iv) may proceed with the stereoselective formation of epoxides, which represent valuable intermediates for stereoselective synthesis. Consequently, halohydrin dehalogenases have been intensely investigated with respect to their mechanism of action and the stereochemical consequences [5] [7].

### 1.4.1 Hydrolytic dehalogenation



For the nucleophilic displacement of halide by a hydroxyl anion catalyzed by  $\alpha$ -haloacid dehalogenase, no cofactor is needed and the halogen is substituted by water as nucleophile yielding the corresponding alcohol as product. Many  $\alpha$ -haloacid dehalogenases have been isolated from different organisms (mostly bacteria) like *Moraxella sp.*, *Pseudomonas sp.* or *Xanthobacter autotrophicus*. [6]

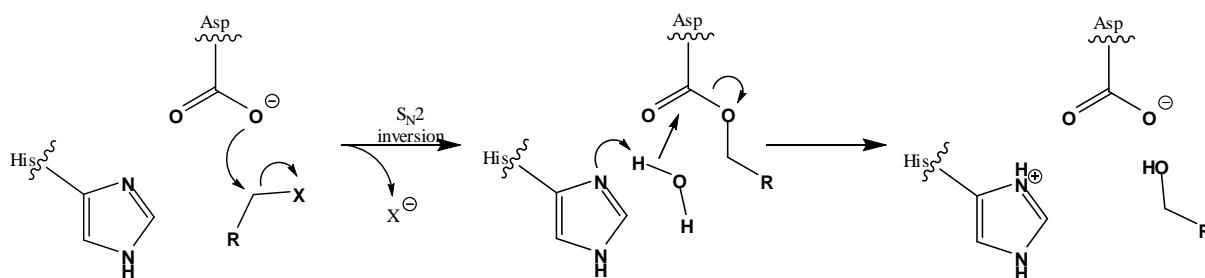
The enzymatic dehalogenation by dehalogenases proceeds via formal nucleophilic substitution, where the halogen atom is replaced by a hydroxyl group. The enzymatic activity is independent of cofactors and metal ions. Previously, it was assumed, that the displacement can be achieved by retention or inversion of configuration, depending on the type of enzyme. Later, however, it was proven that the (assumed) retention was based on erroneous interpretation of data and today it is generally accepted that the enzyme-catalysed nucleophilic displacement of halide generally proceeds with inversion of configuration [16]. This stereospecific property is responsible for the growing interest for synthetic applications. Dehalogenases are grouped into the following subtypes (table 3).

**Table 3** Specificities of enzyme subtypes of dehalogenases

Substrate	Enzyme subtype	Specificity
Alkyl-halide	Haloalkane dehalogenase	Low
Aryl-halide	Haloaromatic dehalogenase	Low
$\alpha$ -Haloacid	$\alpha$ -Haloacid dehalogenase	High

As shown in Table 3, haloalkane dehydrogenases are thought to have a low substrate specificity, which is due to the fact, that they are mainly involved in biodegradation. In the course of this work, it will be shown, that this is not always the case and that there are exceptions.

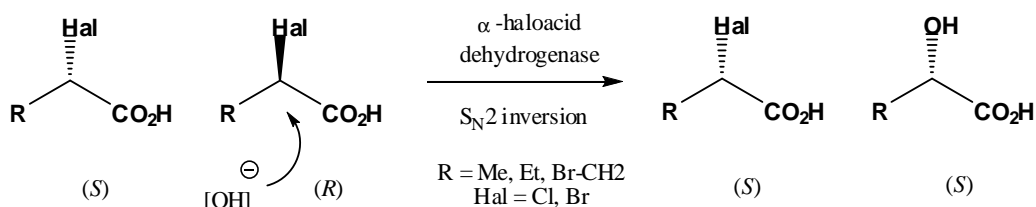
In relation to the mechanism, haloalkane dehydrogenases are very similar to epoxide hydrolases, provided that the substitution proceeds under inversion of configuration. The first step in catalysis is the nucleophilic attack of an Asp-carboxylate group on the haloalkane, forming an activated alkyl-ester enzyme intermediate (Scheme 2). The latter is hydrolyzed by a water molecule, which is activated by a histidine group, which forms the corresponding alcohol as hydrolysis product and liberates the Asp-carboxylate to close the catalytic cycle. [5]



**Scheme 2** Mechanism of haloalkane dehalogenases by inversion of configuration with X = Cl, Br, I [5]

The enzyme from *Xanthobacter autotrophicus* is the best understood and most studied dehalogenase. This enzyme of the  $\alpha/\beta$  hydrolase family builds up a catalytic triad with a histidine and an aspartate as nucleophile, which substitutes the halogen from the substrate. The cleavage of the C-X bond is additionally supported by (variable) phenylalanine or asparagine residues and a conserved tryptophan. [6] [7]

Two types of  $\alpha$ -haloacid dehalogenases are known: 2-Haloacid dehydrogenases and haloacetate dehydrogenases. While 2-haloacid dehalogenases are accepting various types of short-chain 2-haloacids as substrate, haloacetate dehalogenases prefer only haloacetate.

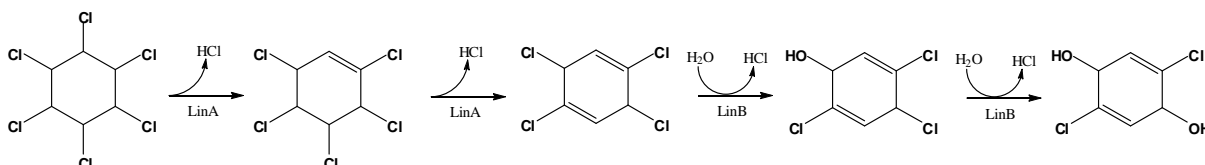


**Scheme 3** Biotransformation of  $\alpha$ -haloacids by 2-haloacid dehalogenase with inversion of configuration

The most interesting facette of dehalogenases is their enantioselectivity shown in scheme 3. Historically, the major reference for that kind of substrate is 2-chloropropionic acid. Its (*S*)-enantiomer is used for a wide range of synthetic applications, most prominently in the sector of herbicides. With the use of (*R*)-specific dehalogenases, the racemic substrate can be converted to the pure (*S*)-enantiomer in a very elegant way. For getting access to other substrates, like long-chain  $\alpha$ -haloacids or

hydrolytically sensitive substrates, other solvents like anhydrous organic ones could be used. [5]

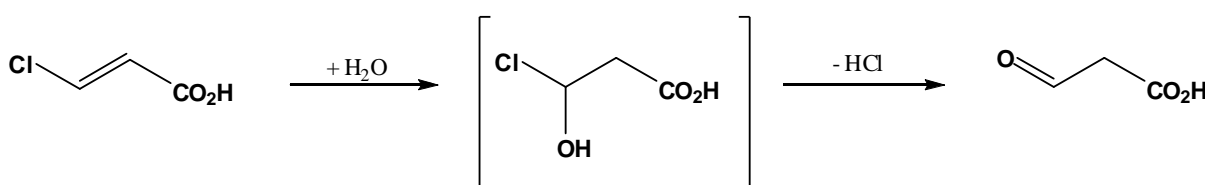
The enzyme LinB, which is of major interest in this work, is a good example for a haloalkane dehalogenase. LinB catalyzes the dehalogenation of e.g. tetrachlorocyclohexadiene, which is an intermediate in the dehalogenation of  $\gamma$ -hexachlorocyclohexane, also called lindane (scheme 4). [7]



**Scheme 4** Dehalogenation steps of lindane by LinA (dehydrohalogenation) and LinB (hydrolytic dehalogenation)

Hexachlorocyclohexane (HCH) and technical mixtures of HCH ( $\alpha$ -,  $\beta$ -,  $\gamma$ - and  $\delta$ -) have been produced worldwide for their insecticide activity. Nowadays, many countries have banned its use due to its toxicity and persistence. One organism, which is able to degrade HCH is *Sphingomonas paucimobilis*, which uses HCH as carbon- and energy source. [8]

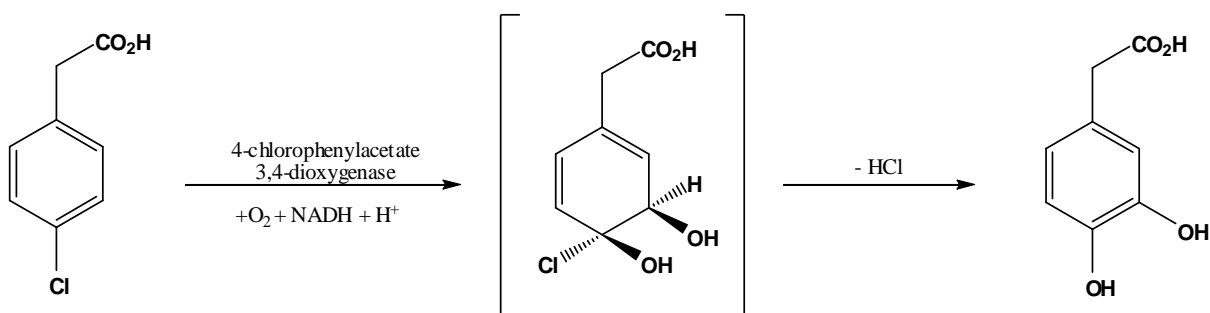
The hydrolytic degradation of  $\beta$ -chloroacrylate is believed to occur via enzyme-catalyzed hydration of the activated (conjugated) C=C bond via addition of water, to form an unstable intermediate, which collapses through HCl elimination with formation of malonate semialdehyde, as shown in scheme 5. [6]



**Scheme 5** Enzymatic dehalogenation of  $\beta$ -haloacrylate via hydration - dehydrohalogenation sequence

### 1.4.2 Oxidative dehalogenation

As substrates for enzymatic oxidative dehalogenation, haloaromatic compounds as well as haloaliphatic analogs are accepted. Monooxygenases, like methane monooxygenase, or dioxygenases (scheme 6) have to be mentioned. But also lignin and manganese peroxidase are involved in these processes.



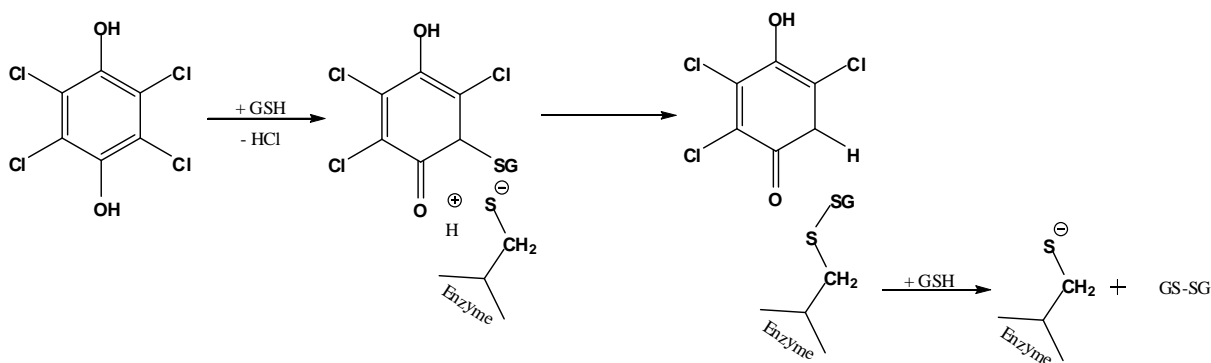
**Scheme 6** Two component system for oxidative dehalogenation

### 1.4.3 Reductive dehalogenation

This kind of dehalogenation can proceed either under aerobic or anaerobic conditions.

#### i) Aerobic conditions

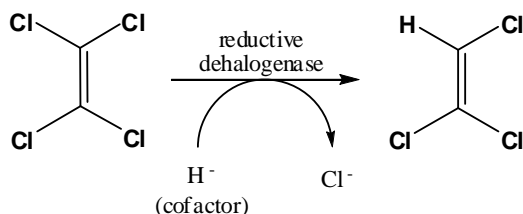
One well-understood reductive dehalogenation is the dehalogenation of pentachlorophenol. The first step is catalyzed by a pentachlorophenol hydroxylase (monooxygenase reaction) yielding a tetrachloroquinone, which is further dehalogenated by tetrachloroquinone dehalogenase giving the trichloroquinone as product (Scheme 7). Tetrachloroquinone dehalogenase belongs to the family of glutathione transferases.



**Scheme 7** Glutathione transferase catalyzed reductive dehalogenation under aerobic conditions

ii) Anaerobic conditions

In this case, the halogenated substrate acts as an electron acceptor while an electron-rich reactant is oxidized. This reaction type depends on cofactors like cobalamin and iron-sulfur clusters, e.g. as shown for the reductive dehalogenase from *Dehalococcoides ethenogenes* (Scheme 8). This kind of dehalogenation is strongly coupled to energy metabolism. [6]



**Scheme 8** Reductive dehalogenation of tetrachloroethene under anaerobic conditions

Up to date, there are three different types of reductive dehalogenases known.

- Trichloroethene reductive dehalogenase (*Dehalococcoides ethenogenes*)
- Tetrachloroethene reductive dehalogenase (*Dehalospirillum multivorans*)
- *ortho*-Chlorophenol reductive dehalogenase (*Desulfitobacterium dehalogenans*)

Trichloroethene reductive dehalogenase substitutes each halide step by step ending up with ethene after three consecutive cycles. This enzyme also accepts 1,2-dichloroethane and 1,2-dibromoethane. With genome sequencing it has been shown that there may be more different types of dehalogenases present in *Dehalococcoides ethenogenes*. [7]

## Haloalkane dehalogenase LinB

Haloalkane dehalogenase like LinB from *Sphingomonas paucimobilis* are detoxifying enzymes which are accepting a wide scope of halogenated compounds. The product is the corresponding alcohol. The haloalkane dehalogenase catalyzes the substitution of a halide in primary or secondary position with a hydroxyl group. [9] LinB is a compact globular enzyme from the  $\alpha/\beta$ -hydrolase family. Other members of this family are e.g. lipases, acetylcholine esterases, epoxide hydrolases, serine carboxypeptidases and many more. All these proteins contain a catalytic triad with a nucleophilic carboxylate. The histidine residue is supporting the H<sub>2</sub>O-activation. The most conserved structural characteristic of haloalkane dehydrogenases is a nucleophilic elbow and a central  $\beta$ -sheet. The hydrophobic core which includes the catalytic triad of aspartate-histidine-aspartate/glutamate represents the main domain. [11]

The first step is the binding of the lipophilic substrate in a hydrophobic pocket. The nucleophilic attack of aspartate anion onto the carbon bearing the halogen atom is the next step, which yields a covalent alkyl-enzyme intermediate. The latter is further hydrolyzed with water which is activated by a histidine residue acting as a base. [9] Another aspartate (or glutamate) acts as acid to stabilize the charge of the imidazole ring of the histidine during the hydrolytic half reaction. [11] By formation of an alkyl-ester enzyme-intermediate bound to aspartate, the halide is liberated. [10] Kinetic studies showed that product release is the rate-determining step.

The substrate spectrum of LinB is rather broad. A wide range of halo-alkanes as well as -alkenes, halogenated cyclic dienes, like 1,3,4,6-tetrachlorohexadiene-1,4-diol, which occur as intermediates in HCH dechlorination (scheme 7), are accepted in the reaction, which is independent on a cofactor or oxygen. [9] The binding of 1,2-dichloroethane (1,2-DCE) and 1,2-dichloropropane (1,2-DCP) results in the inhibition of the enzyme. While 1,2-DCE is produced in many industrial processes, 1,2-DCP arises as a side product from the synthesis of epichlorohydrin and propene oxide. Since 1,2-DCP and 1,2-DCE are not converted by haloalkane dehalogenases, they represent problematic and recalcitrant pollutants. [10]

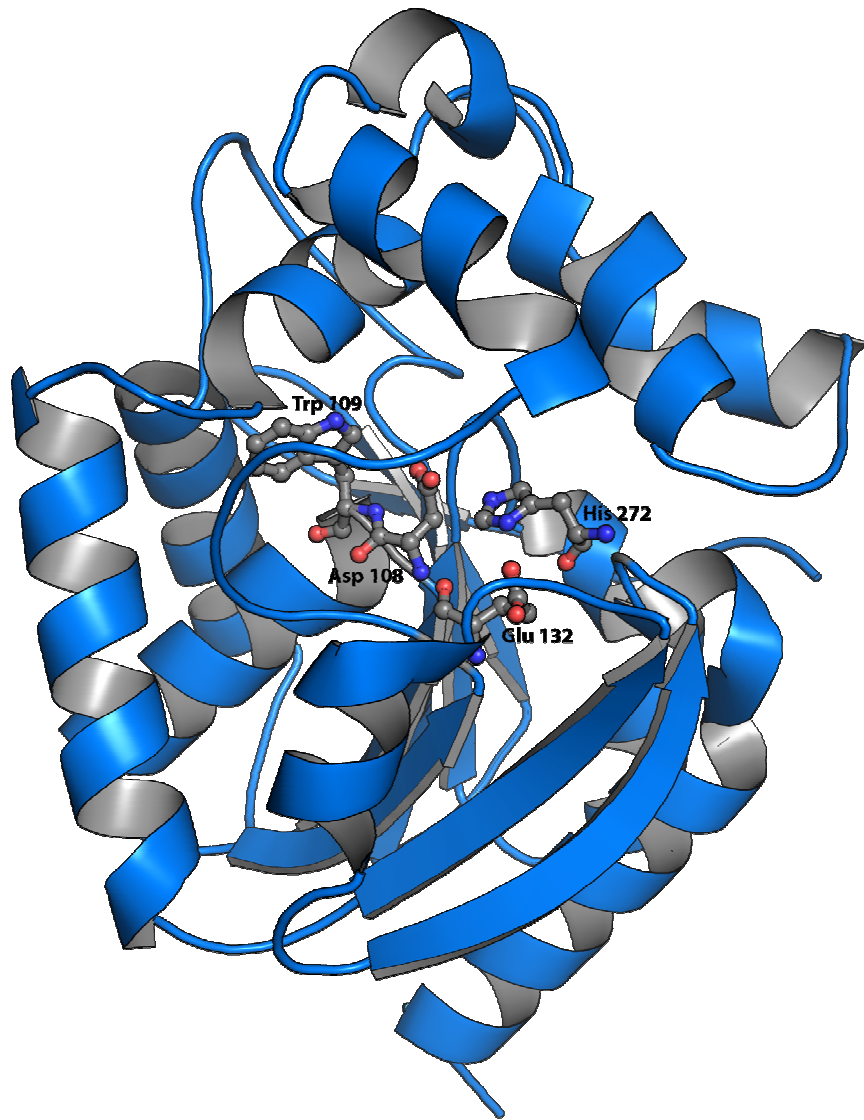


**Fig. 4** 3D-Structure of the enzyme LinB (PDB entry 1CV2);

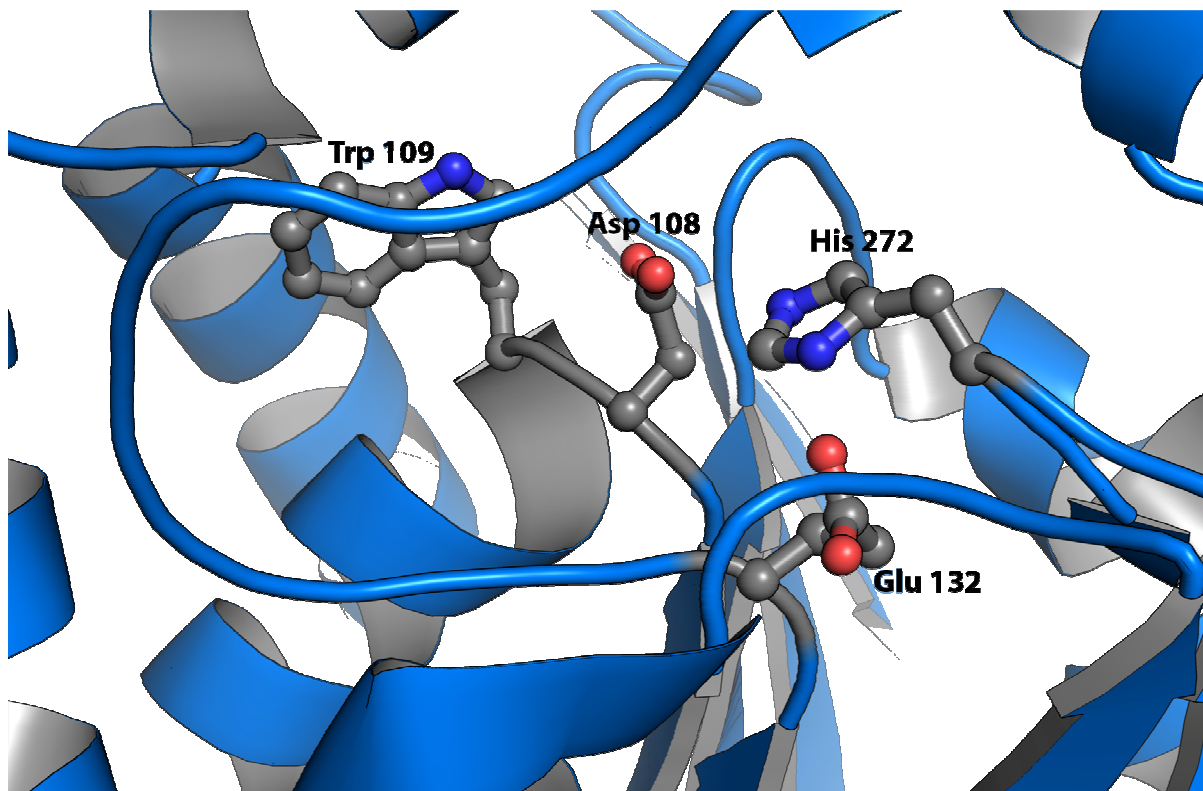


**Fig. 5** Zoom of the active site, built up by Glu 132, His 272, Asp 108 and Trp 109 residues.

## 2. Results and Discussion

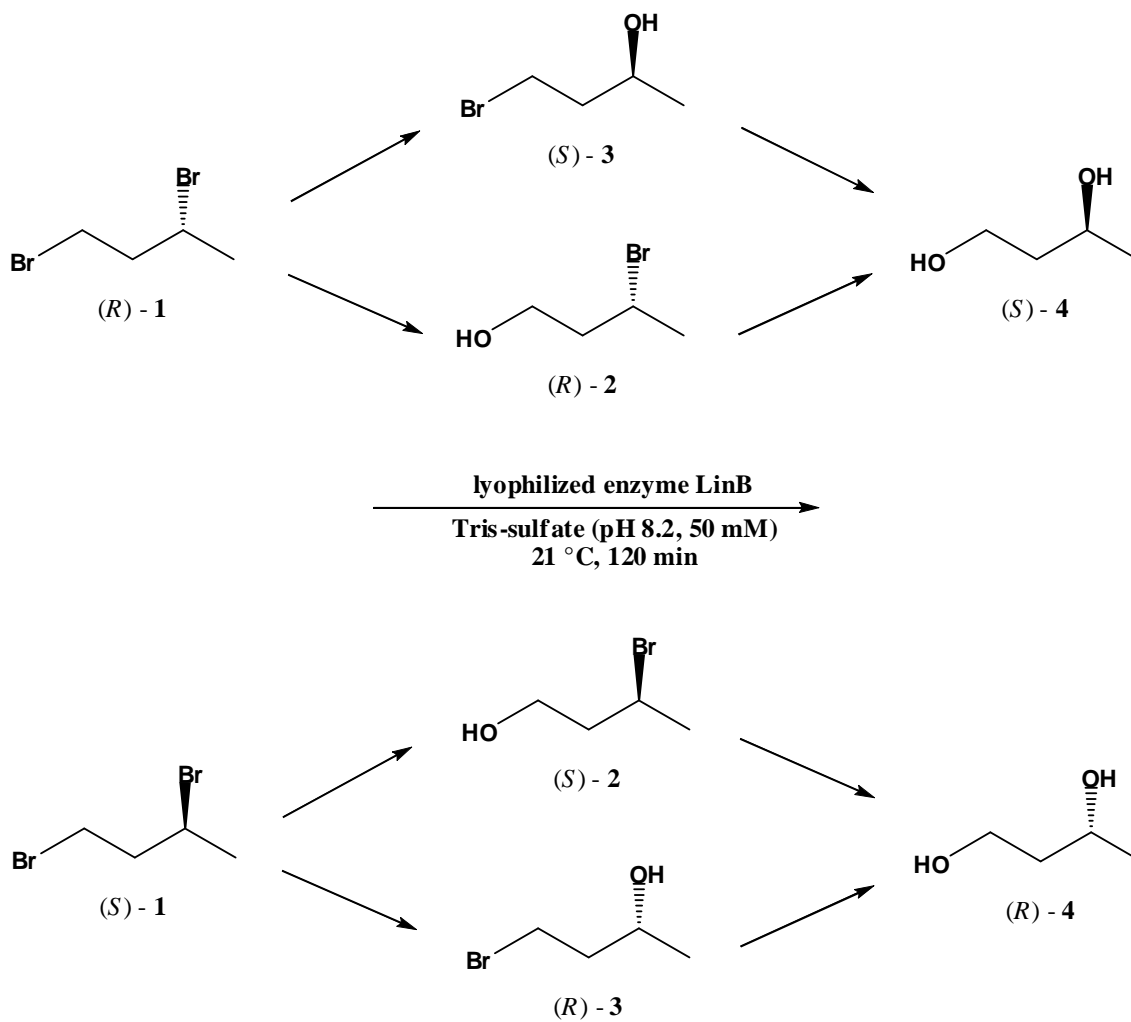


**Fig. 5** Regio- and stereoselective sequential enzymatic dehalogenation of *rac*-1,3-dibromobutane by LinB

## 2.1 General

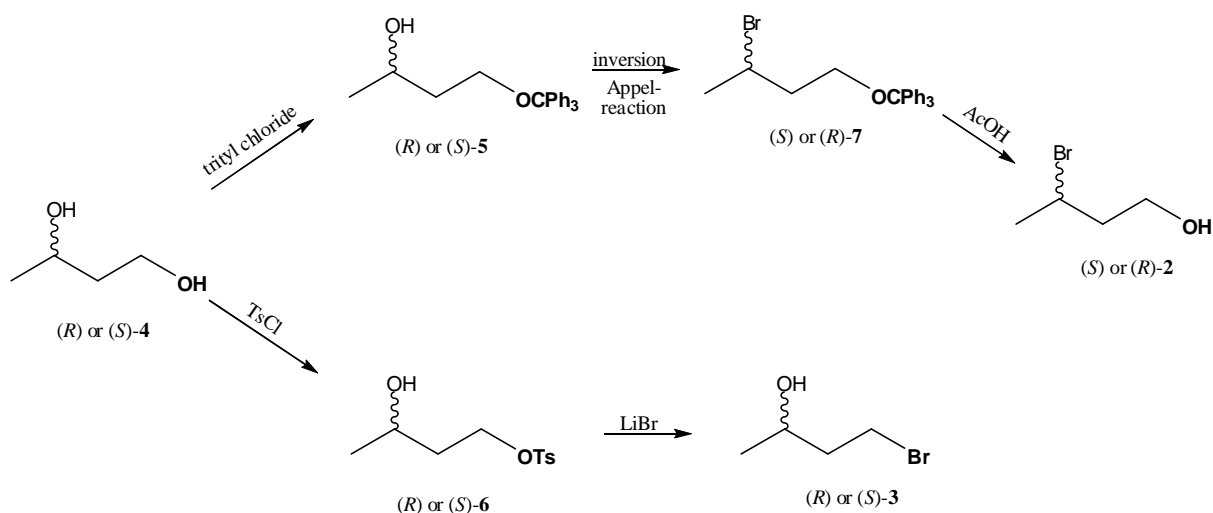
Based on preliminary studies carried out at the University of Brno, Czech Republic, the dehalogenation of *rac*-1,3-dibromobutane (*rac*-**1**) was investigated using LinB in Tris-sulfate buffer at pH 8.2 and room temperature (21 °C). In principle, there are two reaction pathways possible (Fig. 5):

Depending on the regioselectivity of the enzyme i.e. the preference of the enzyme for the replacement of the *prim*- or the *sec*-halogen atom, products **2** or **3** would be formed. During replacement of the *prim*-halogen, the configuration of the remaining *sec*-halogen would be retained [i.e. (*R*)-**1** → (*R*)-**2** and (*S*)-**1** → (*S*)-**2**], while reaction of the *sec*-halogen atom would proceed with inversion [i.e. (*R*)-**1** → (*S*)-**3** and (*S*)-**1** → (*R*)-**3**]. Analogous considerations are applicable to the second step, i.e. retention takes place from (*S*)-**3** → (*S*)-**4** and (*R*)-**3** → (*R*)-**4**. Inversion occurs from (*R*)-**2** → (*S*)-**4** and (*S*)-**2** → (*R*)-**4**, respectively. Overall, during the first step, kinetic resolution of *rac*-**1** takes place, going in hand with the formation of four different products, i.e. enantiomeric pairs of two different regio-isomeric halo-alcohols **2** and **3**. In the second step, two enantiomeric pairs of regio-isomers are kinetically resolved to yield one pair of enantiomers of the final hydrolysis product **4**. The distribution of each enantiomeric isomer **2**, **3** and **4** depends on the relative rate constants of each step.

The major task of this work was to determine the absolute configuration of the intermediates **2** and **3** and of the final product **4** as well as which enantiomer of substrate **1** is preferred by the enzyme LinB. While *rac*-**1**, (*S*)-**4** and (*R*)-**4** were commercially available, the intermediates (*S*)-**3**, (*R*)-**3**, (*S*)-**2** and (*R*)-**2** had to be independently synthesized.

## 2.2 Synthesis of (*S*)-3 and (*R*)-3

In order to access the enantiomers of halo-alcohol **3**, the primary alcohol functionality of diols (*R*)-**4** and (*S*)-**4** was activated with *p*-toluenesulfonyl chloride in pyridine on ice as a good leaving group, which selectively occurs at the sterically less hindered *prim*-hydroxy group, to yield the corresponding *mono*-tosylates (*R*)-**5** and (*S*)-**5**.



**Scheme 9** Schematic overview of synthesis of (*R*)- and (*S*)-**3** as well as (*R*)- and (*S*)-**2**

In a subsequent step, the tosylate was easily replaced by bromide using LiBr in DMF at room temperature, to furnish (*S*)-**3** and (*R*)-**3**.

## 2.3 Synthesis of (*S*)-2 and (*R*)-2

For the synthesis of (*S*)-**2** and (*R*)-**2**, the same starting materials (*S*)-**4** and (*R*)-**4** were used. First, the primary alcohol moiety was protected with trityl chloride in pyridine at room temperature, which prefers the *prim*-hydroxy group with excellent regioselectivity. For the substitution of the remaining non-converted hydroxyl group in the secondary position by bromide, the Appel-protocol was chosen. [14] With carbon tetrabromide and triphenylphosphine in dichloromethane at room temperature, this reaction proceeded with inversion of configuration. Finally, the trityl protecting group was carefully cleaved under mild acidic conditions with acetic acid at 50 °C yielding (*R*)-**2** and (*S*)-**2** from (*S*)-**4** and (*R*)-**4**, respectively.

With these independently synthesised standard materials in hand, the GC-peaks for the intermediate **2** and **3** and the final product **4** could be annotated with respect to their absolute configuration.

## 2.4 Kinetic resolution of 1,3-dibromobutane

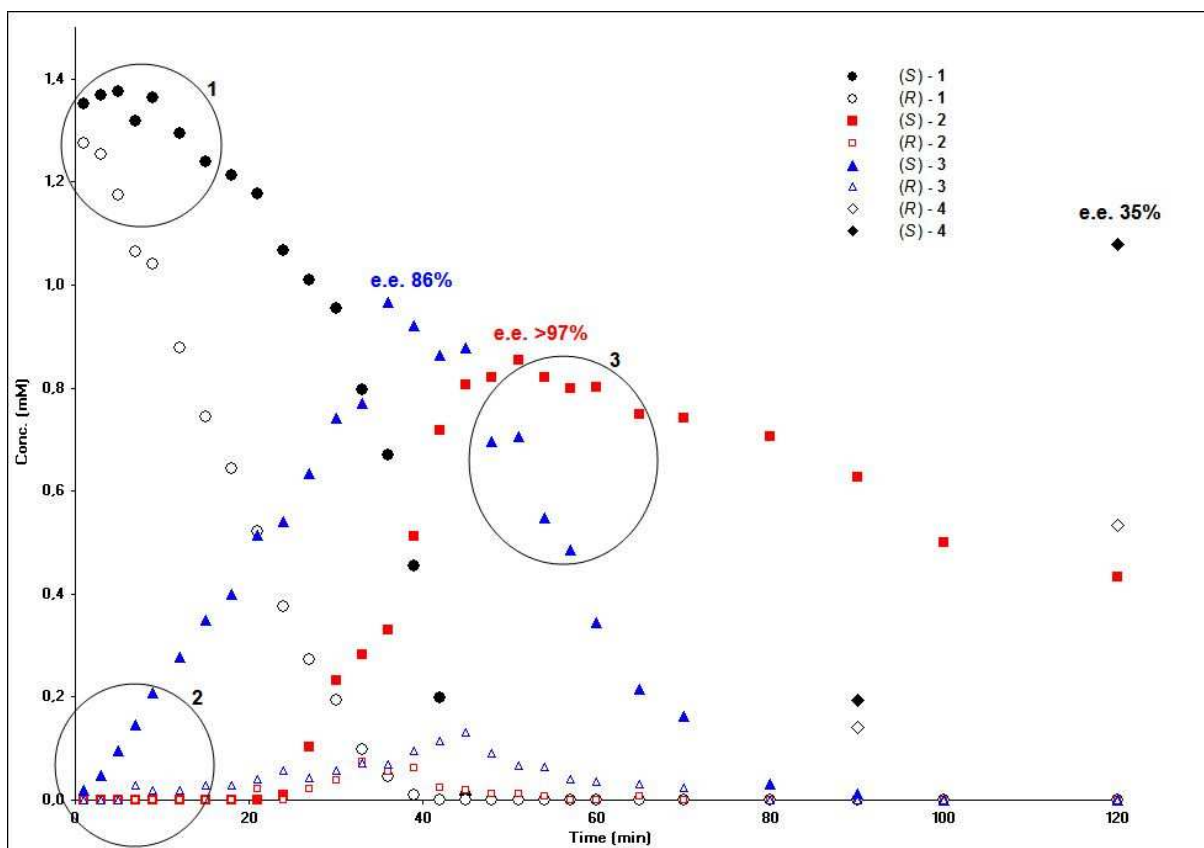


**Fig. 6** amounts of intermediates depending to the time provided by the group of Zbynek Prokop - University of Brno, Czech Republic; data from 4 were taken from a separate experiment, whereby different reaction rates explain the non-close mass balance.

Figure 6 shows that the first mainly formed intermediate after 10 minutes is (S)-**3** with an e.e. >99%, which means that the substrate enantiomer preferred by LinB is (R)-**1**, because hydrolysis of the *sec*-halogen atom occurs with inversion of configuration. The k-value of this particular step is 68  $\mu\text{mol}/\text{min}$  and is the highest of the whole reaction. After 30 minutes, the velocity of the hydrolysis of **1** slows down somewhat and the e.e. of (S)-**3** decreases to about 80 %, which can be expected in a kinetic resolution, when

the good-fitting (*R*)-enantiomer of **1** is gradually depleted (to an e.e. of 30% at 30 minutes) and the mirror-image is increasingly converted. The k-values of (*S*)-**2** and (*S*)-**3** are nearly the same.

After 40 minutes, the e.e. of (*S*)-**1** is higher than 90 % which means, that the preferred (*R*)-enantiomer is almost completely converted. At this point, all intermediates [except (*S*)-**2**, whose ee-value is still rising] are at the peak. The k-values of (*S*)-**3** and (*R*)-**2** after 60 minutes confirm that the reaction from (*S*)-**3** to (*S*)-**4** is dominant and the fastest from the intermediate to the final product.

While k-values are decreasing, after 90 minutes (*S*)-**4** is formed with an e.e. of about 15 %. Due to the good water-solubility of **4**, its amount could not be accurately determined but only be calculated by taking the difference of **1**, **2** and **3** to the total amount of compounds of 100 %. Diol (*S*)-**4** is formed more than twice as fast as (*R*)-**4** and after 120 minutes the e.e.-value of (*S*)-**4** is 35%. The amounts of all intermediates are given in figure 6.

## Conclusion

LinB prefers the (*R*) enantiomer of the substrate **1** for hydrolysis of the *sec*-halogen atom. The initial rate of (*R*)-**1** is about 5 times higher than (*S*)-**1** (figure 6, marked as "1").

As consequence, intermediate (*S*)-**3** is formed faster than (*S*)-**2** (figure 6, marked as "2"). Actually, the stereo-preference for the *sec*-bromide is (*R*)-**1** => (*S*)-**3** where (*S*)-**3** has an e.e. <sub>max</sub> of 86%.

The stereo-preference for the *prim*-bromide is (*S*)-**1** => (*S*)-**2** where (*S*)-**2** has an e.e. <sub>max</sub> of >97%.

The initial rate of (*S*)-**3** => (*S*)-**4** is about 5 times faster than (*S*)-**2** => (*R*)-**4** (figure 6, marked as "3"), thus yielding in the final product (*S*)-**4**, as shown in figure 7, with an e.e. <sub>max</sub> of 35%.

### **3. Experimental**

#### **3.1 General**

All chemicals, substrates and reference materials were used without further purification and were purchased from Sigma Aldrich, Fluka and Lancaster. All solvents were purchased from Roth. Solvents marked "anhydrous" were dried over molecular sieve 4 Å. Anhydrous THF was distilled over sodium/benzophenone. Enzyme LinB was provided by the group of Z. Prokop (University of Brno, Czech Republic).

All biotransformations and rehydration of protein were done in Eppendorf tubes (1.5 mL) mounted in a horizontal position on a HT Infors Unitron shaker AJ 260 at 120 rpm and 21 °C. Centrifugation was done in a Hareaeus Biofuge pico at 13.000 rpm at room temperature.

NMR spectra were recorded in CDCl<sub>3</sub> as solvent with 0.03 % TMS as internal standard. The spectrum recording was done on a Bruker NMR unit at 300 MHz. Chemical shifts are reported in ppm and coupling constants in Hz as unit.

GC-MS analyses were recorded on a Agilent Technologies 7890A GC-System coupled with an Agilent Technologies 5975C inert XLMSD detector using a HP-5MS column.

GC-FID on a chiral stationary phase were carried out with an Agilent Technologies 7890A GC-system using Hydrodex ® -β-TBPAC 50 m column.

TLC analyses were carried out on silica gel 60 F<sub>254</sub> sheets from Merck. As spray reagent cerium ammonium molybdate/H<sub>2</sub>SO<sub>4</sub> was used.

#### **3.2 Enzyme LinB**

Enzyme LinB was prepared as reported in literature [18]. The enzyme (10 mg/mL) in phosphate buffer (50 mM, pH 7.5) was lyophilized and used as such in further reactions.

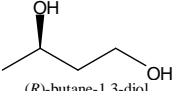
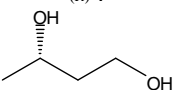
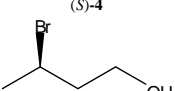
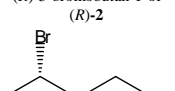
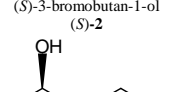
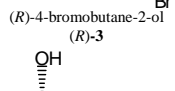
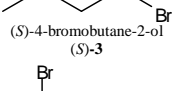
### 3.3 General Procedure for Biotransformation

To 20 mL Tris-buffer (pH 8.2, 50 mM) in 50 mL Sarstedt tubes was added *rac*-1,3-dibromobutane (12  $\mu$ L, 5 mM). Then, LinB (500  $\mu$ L from a stock solution containing 1.5 mg/mL, final concentration 37.5  $\mu$ g/mL) was added and the solution was incubated with shaking for 120 min at 21  $^{\circ}$ C and 120 rpm.

The reaction was stopped by saturating the solution with NaCl and the products were extracted twice with ethyl acetate (10 mL). After separation of the phases, the combined organic layers were dried over NaSO<sub>4</sub> and transferred into GC-glass-vials.

### 3.4 Analytical Data

**Table 4** Overview of analytical R<sub>f</sub> data and retention times

compound	GC-MS retention time [min]	GC-MS-method/column	GC-FID retention time [min]	GC-FID method/column	TLC-method/R <sub>f</sub>
 ( <i>R</i> )-butane-1,3-diol ( <i>R</i> )-4	5.89	A / A	15.55	B / B	C / 0.10
 ( <i>S</i> )-butane-1,3-diol ( <i>S</i> )-4	5.89	A / A	14.93	B / B	C / 0.10
 ( <i>R</i> )-3-bromobutan-1-ol ( <i>R</i> )-2	6.45	A / A	13.90	B / B	C / 0.48
 ( <i>S</i> )-3-bromobutan-1-ol ( <i>S</i> )-2	6.45	A / A	13.55	B / B	C / 0.48
 ( <i>R</i> )-4-bromobutane-2-ol ( <i>R</i> )-3	6.22	A / A	13.30	B / B	C / 0.50
 ( <i>S</i> )-4-bromobutane-2-ol ( <i>S</i> )-3	6.22	A / A	12.72	B / B	C / 0.50
 1,3-dibromobutane 1	n.d.	A / A	8.40	B / B	n.d.

n.d. = not determined.

**Method A:** Initial temperature 70 °C, hold for 2 minutes, heating with 20 °C/min to 240 °C; split: 90:1; flow: 0.5 mL/min; inlet temperature: 250 °C; pressure gas: 3.14 psi.

**Column A:** HP-5MS; 30 m x 0.25mm, 0.25µm film.

**Method B:** Initial temperature 130 °C, hold for 7 minutes; heating with 5 °C/min to 135 °C and hold for 5 minutes; heating with 5 °C/minutes to 140 °C and hold for 5 minutes; heating with 10 °C/min to reach finally 170 °C.

**Column B:** Hydrodex ® -β-TBPAC (50 m x 0.125 mm, 0.12 µm film).

**TLC method C:** petroleum ether / ethyl acetate 2:1.

### 3.5 GC-FID detector calibration

Due to the different response factors of reference materials, a calibration with compounds **1**, **2**, **3** and **4** was performed. By theory, the response factors of enantiomers (*R*) and (*S*) are identical. The results are given in figure 7.

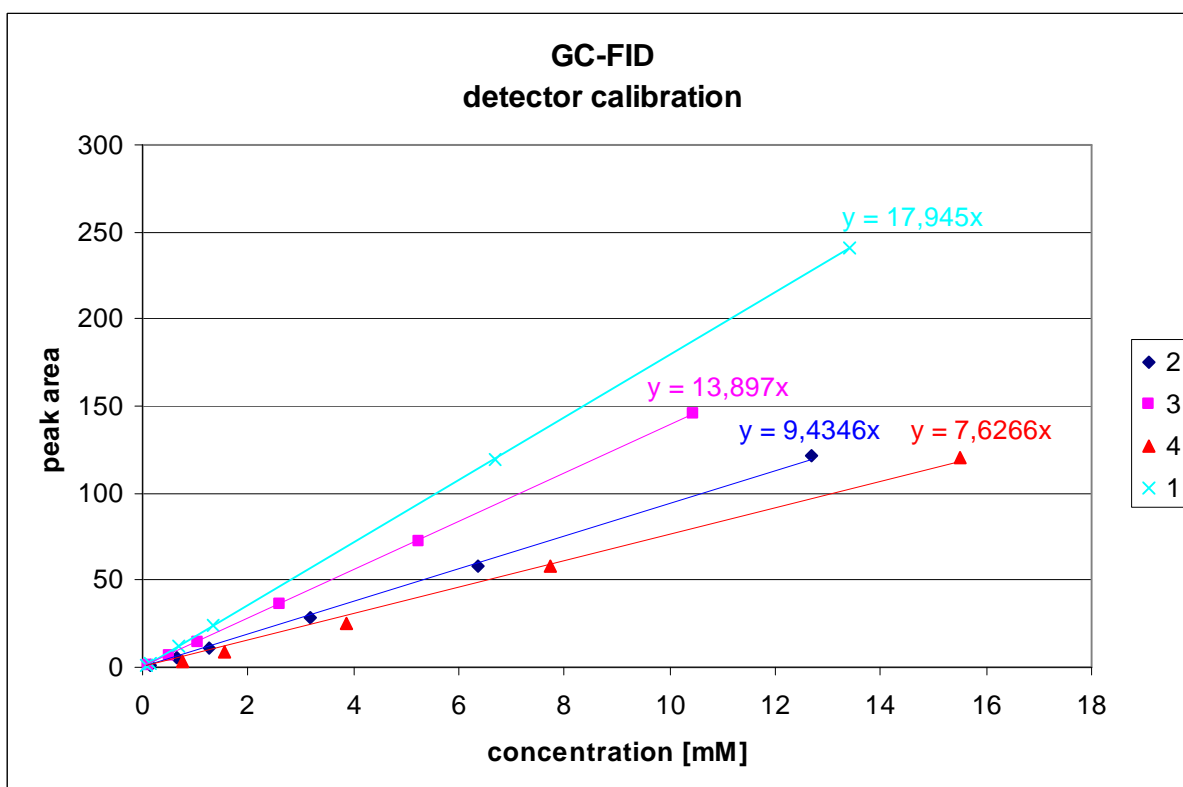
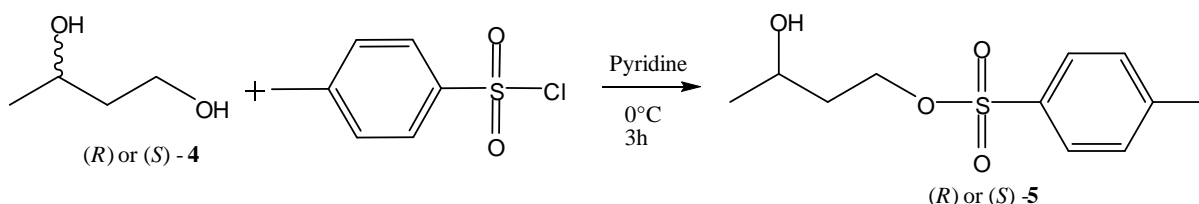


**Fig. 7** GC Calibration curves of compounds **1**, **2**, **3** and **4**

## 3.6 Synthesis

### 3.6.1 Synthesis of 3-hydroxybutyl 4-methylbenzenesulfonate (5)

For protecting the primary hydroxyl group of **1**, the sequences given in scheme 10 were used.



**Scheme 10** Synthesis of (*R*)-3-hydroxybutyl-4-methylbenzenesulfonate [(*R*)-5] [12]

To a solution of (*R*)-**4** respectively (*S*)-**1** (200 mg, 2.22 mmol) in pyridine (1.5 mL) cooled on ice (0 °C) *p*-toluenesulfonyl chloride (472 mg, 2.48 mmol) was added. After stirring for 3 hours, the reaction mixture was diluted with water and extracted with diethyl ether (three times with 10 mL). The organic layer was washed with saturated CuSO<sub>4</sub>-solution and dried over NaSO<sub>4</sub>. After solvent evaporation under reduced pressure, the product was purified by chromatography on silica gel with hexane/ethyl acetate (2:1) to give a yield of 305 mg (56 %) for (*R*)-**5** and 327 mg (60 %) for (*S*)-**5**.

(*R*)-**5**:

TLC R<sub>f</sub> = 0.60 (petroleum ether / EtOAc) 1:2

GC-MS: RT = 13.8 min, m/z [fragment] 229.0 [C<sub>10</sub>H<sub>13</sub>O<sub>4</sub>S]<sup>+</sup>, 185.0 [C<sub>8</sub>H<sub>9</sub>O<sub>3</sub>S]<sup>+</sup>, 172.1 [C<sub>7</sub>H<sub>7</sub>O<sub>3</sub>S]<sup>+</sup>, 155.1 [C<sub>7</sub>H<sub>7</sub>O<sub>2</sub>]<sup>+</sup>, 91.1 [C<sub>7</sub>H<sub>7</sub>]<sup>+</sup>

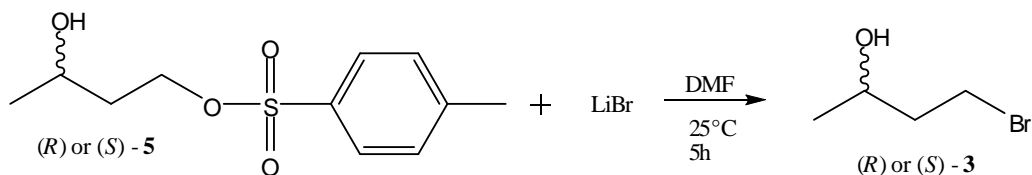
(*S*)-**5**:

TLC R<sub>f</sub> = 0.60 (petroleum ether / EtOAc) 1:2

GC-MS: RT = 13.8 min, m/z [fragment] 229.0 [C<sub>10</sub>H<sub>13</sub>O<sub>4</sub>S]<sup>+</sup>, 185.0 [C<sub>8</sub>H<sub>9</sub>O<sub>3</sub>S]<sup>+</sup>, 172.1 [C<sub>7</sub>H<sub>7</sub>O<sub>3</sub>S]<sup>+</sup>, 155.1 [C<sub>7</sub>H<sub>7</sub>O<sub>2</sub>]<sup>+</sup>, 91.1 [C<sub>7</sub>H<sub>7</sub>]<sup>+</sup>

### 3.6.2 Synthesis of 4-bromobutane-2-ol (**3**)

For substituting the tosyl protecting group, against bromide, the sequence given in Scheme 11 was used.



**Scheme 11** Synthesis of (*R*) and (*S*)-4-bromobutane-2-ol [(*R*) and (*S*)-**3**] [13]

To a solution of **5** [305 mg, 1.25 mmol (*R*)-**5**; 327 mg, 1.34mmol (*S*)-**5**] in dry DMF (600  $\mu$ L) lithium bromide (163 mg, 1.87 mmol) was added. After stirring at room temperature for 5 hours the reaction mixture was diluted with a small amount of water and extracted with diethyl ether (three times with 10 mL). The organic layer was washed with water and brine, dried over NaSO<sub>4</sub> and concentrated under reduced pressure. The product was purified by chromatography on silica gel with hexane/ethyl acetate (1:1) to give a yield of 74 mg (39 %) for (*R*)-**3** and 82 mg (40 %) for (*S*)-**3**.

(*R*)-**3**:

TLC R<sub>f</sub> = 0.50 (petroleum ether / EtOAc) 2:1

<sup>1</sup>H-NMR:  $\delta$  = 1.27 - 1.25 (d, 3 H, *J* = 6.24 Hz), 1.76 - 1.65 (s, 1 H), 2.05 - 1.95 (m, 2 H), 3.61 - 3.48 (m, 2 H), 4.03 - 3.99 (m, 1 H)

<sup>13</sup>C-NMR:  $\delta$  = 66.1, 41.5, 30.4, 23.5

GC-MS: RT = 6.22 min, m/z [fragment] 150.9/152.9 [C<sub>4</sub>H<sub>7</sub>Br]<sup>+</sup>, 137.0/139.0 [C<sub>3</sub>H<sub>5</sub>Br]<sup>+</sup>, 106.9/108.9 [C<sub>2</sub>H<sub>4</sub>Br]<sup>+</sup>, 92.3/94.3 [CH<sub>2</sub>Br]<sup>+</sup>, 79.0/81.0 [Br]<sup>+</sup>, 73.1 [C<sub>4</sub>H<sub>9</sub>O]<sup>+</sup>, 45.1 [C<sub>2</sub>H<sub>5</sub>O]<sup>+</sup>,

(*S*)-**3**:

TLC R<sub>f</sub> = 0.50 (petroleum ether / EtOAc) 2:1

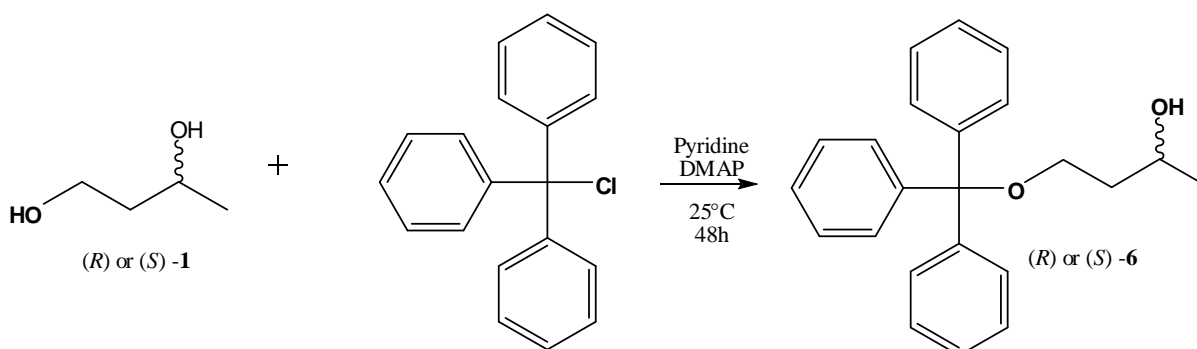
<sup>1</sup>H-NMR:  $\delta$  = 1.27 - 1.25 (d, 3 H *J* = 6.24 Hz), 1.64 - 1.40 (s, 1 H), 2.02 - 1.71 (m, 2 H), 3.61 - 3.48 (m, 2 H), 4.05 - 4.01 (m, 1 H)

<sup>13</sup>C-NMR:  $\delta$  = 66.06, 41.50, 30.40, 23.52

GC-MS: RT = 6.22 min, m/z [fragment] 150.9/152.9 [C<sub>4</sub>H<sub>7</sub>Br]<sup>+</sup>, 137.0/139.0 [C<sub>3</sub>H<sub>5</sub>Br]<sup>+</sup>, 106.9/108.9 [C<sub>2</sub>H<sub>4</sub>Br]<sup>+</sup>, 93.0/95.0 [CH<sub>2</sub>Br]<sup>+</sup>, 79.0/81.0 [Br]<sup>+</sup>, 73.1 [C<sub>4</sub>H<sub>9</sub>O]<sup>+</sup>, 45.1 [C<sub>2</sub>H<sub>5</sub>O]<sup>+</sup>,

### 3.6.3 Synthesis of 4-(triphenylmethoxy)butan-2-ol (**6**)

For protecting the primary hydroxyl group of **1**, the sequence given in Scheme 12 and Scheme 14 was used.



**Scheme 12** Synthesis of (*R*) and (*S*)-4-(triphenylmethoxy)butan-2-ol [(*R*) and (*S*)-**6**] [14]

A solution of **1** (180 mg, 2 mmol) in pyridine (350  $\mu$ L) was added to trityl chloride (631 mg, 2.2 mmol) in pyridine (1.75 mL). DMAP (6 mg, 0.004 mmol) was added and the reaction mixture was stirred for 48 hours at room temperature. After adding water (5 mL, 0  $^{\circ}$ C) the residue was extracted with dichloromethane (three times with 10 mL), dried over NaSO<sub>4</sub> and purified by chromatography on silica gel with hexane/ethyl acetate (2:1) to give a yield of 614 mg (92 %) for (*R*)-**6** and 570 mg (85%) for (*S*)-**6**.

(*S*)-**6**:

TLC R<sub>f</sub> = 0.58 (petroleum ether / EtOAc) 2:1

GC-MS: RT = 18.9 min, m/z [fragment] 332.2 [C<sub>23</sub>H<sub>24</sub>O<sub>2</sub>], 259.1 [C<sub>19</sub>H<sub>15</sub>O]<sup>+</sup>, 255.4 [C<sub>17</sub>H<sub>19</sub>O<sub>2</sub>]<sup>-</sup>, 243.2 [C<sub>19</sub>H<sub>15</sub>]<sup>-</sup>, 89.1 [C<sub>4</sub>H<sub>9</sub>O<sub>2</sub>]<sup>-</sup>, 77.1 [C<sub>6</sub>H<sub>5</sub>]<sup>-</sup>, 73.1 [C<sub>4</sub>H<sub>9</sub>O]<sup>-</sup>,

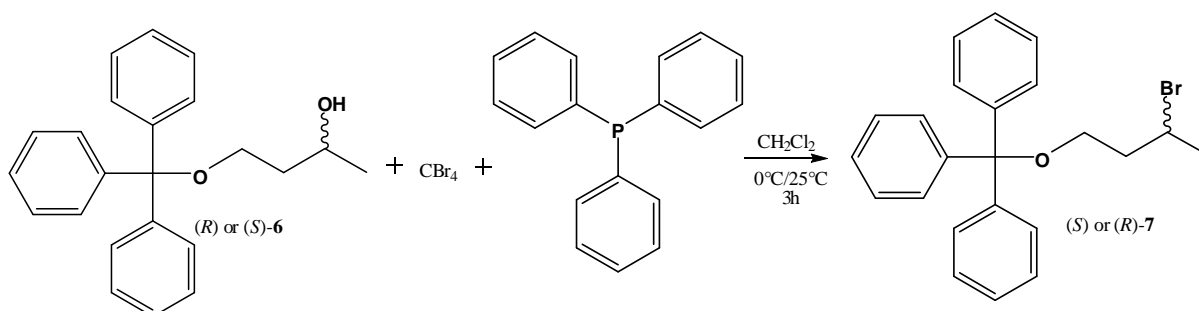
(*R*)-**6**:

TLC R<sub>f</sub> = 0.58 (petroleum ether / EtOAc) 2:1

GC-MS: RT = 18.9 min, m/z [fragment] 332.2 [C<sub>23</sub>H<sub>24</sub>O<sub>2</sub>], 259.1 [C<sub>19</sub>H<sub>15</sub>O]<sup>+</sup>, 255.4 [C<sub>17</sub>H<sub>19</sub>O<sub>2</sub>]<sup>-</sup>, 243.2 [C<sub>19</sub>H<sub>15</sub>]<sup>-</sup>, 89.1 [C<sub>4</sub>H<sub>9</sub>O<sub>2</sub>]<sup>-</sup>, 77.1 [C<sub>6</sub>H<sub>5</sub>]<sup>-</sup>, 73.1 [C<sub>4</sub>H<sub>9</sub>O]<sup>-</sup>,

### 3.6.4 Synthesis of 7

For substituting the alcohol group of (*S*)-**6** and (*R*)-**6** against bromide, the sequence given in Scheme 13 was used. This reaction step proceeds under inversion of configuration.



**Scheme 13** Synthesis of (*R*) and (*S*)-**7** [15]

To a cooled solution on ice of **6** (570 mg, 1.71 mmol (*S*)-**6**; 614 mg, 1.85 mmol (*R*)-**6**) and carbon tetrabromide (623 mg, 1.08 mmol; 670 mg, 2.02 mmol) in dichloromethane (750  $\mu\text{L}$ ; 800  $\mu\text{L}$ ) triphenylphosphine (493 mg, 1.88 mmol; 535 mg, 2.04 mmol) was added over 30 minutes. After stirring for 3 hours at room temperature, hexane (10 mL) was added. The white precipitate was filtered off and the remaining solution was concentrated under reduced pressure. The product was purified by chromatography on silica gel with hexane/ethyl acetate (6:1) to give a yield of 650 mg (95 %).

(*S*)-**7**:

TLC  $R_f = 0.76$  (petroleum ether / EtOAc) 6:1

GC-MS: RT = 19.7 min, m/z [fragment] 394.2/396.2 [ $\text{C}_{23}\text{H}_{23}\text{BrO}$ ], 317.1/319.1 [ $\text{C}_{17}\text{H}_{18}\text{BrO}$ ] $^-$ , 259.1 [ $\text{C}_{19}\text{H}_{15}\text{O}$ ] $^-$ , 243.2 [ $\text{C}_{19}\text{H}_{15}$ ] $^-$ , 135.0/137.0 [ $\text{C}_4\text{H}_8\text{Br}$ ] $^-$ , 77.1 [ $\text{C}_6\text{H}_5$ ] $^-$ ,

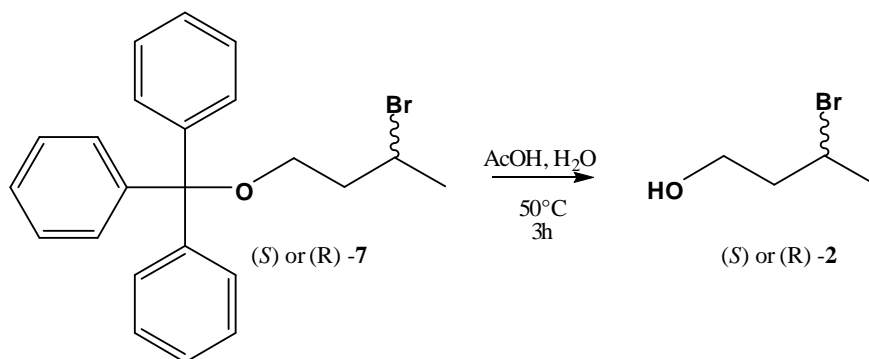
(*R*)-**7**:

TLC  $R_f = 0.76$  (petroleum ether / EtOAc) 6:1

GC-MS: RT = 19.7 min, m/z [fragment] 394.2/396.2 [ $\text{C}_{23}\text{H}_{23}\text{BrO}$ ], 317.1/319.1 [ $\text{C}_{17}\text{H}_{18}\text{BrO}$ ] $^-$ , 259.1 [ $\text{C}_{19}\text{H}_{15}\text{O}$ ] $^-$ , 243.2 [ $\text{C}_{19}\text{H}_{15}$ ] $^-$ , 135.0/137.0 [ $\text{C}_4\text{H}_8\text{Br}$ ] $^-$ , 77.1 [ $\text{C}_6\text{H}_5$ ] $^-$ ,

### 3.6.5 Synthesis of 3-bromobutan-1-ol (2)

The cleavage of the triphenylmethyl ether was done under mild acidic conditions shown in Scheme 14 yielding **2**.



**Scheme 14** Synthesis of (*S*) and (*R*)-3-bromobutan-1-ol [(*S*)-**2** or (*R*)-**2**]

The protected alcohol **7** (540 mg, 1.37 mmol (*S*)-**7**; 650 mg, 1.64 mmol (*R*)-**7**) was dissolved in acetic acid (11 mL) at 50 °C with stirring. Water (1.2 mL) was added and the cloudy solution became clear after stirring for 3 hours at the same temperature. The product was extracted with hexane/ethyl acetate (9:1, three times with 10 mL) and purified by chromatography on silica gel with hexane/ethyl acetate (2:1) to give a yield of 130 mg (62 %) for (*S*)-**2** and 158 mg (63 %) for (*R*)-**2**. [4]

#### (*S*)-**2**

R<sub>f</sub> = 0.48 (petroleum ether / EtOAc) 2:1

<sup>1</sup>H-NMR: δ = 1.77 - 1.75 (d, 3 H, *J* = 6.70 Hz), 2.10 - 1.96 (m, 2 H), 3.85 - 3.81 (m, 2 H), 4.39 - 4.26 (m, 1 H), 7.27 (s, 1 H)

<sup>13</sup>C-NMR: δ = 60.87, 47.99, 43.24, 26.55

GC-MS: RT = 6.45 min, m/z [fragment] 136.0/134.0 [C<sub>4</sub>H<sub>8</sub>Br]<sup>+</sup>, 120.9/122.9 [C<sub>3</sub>H<sub>6</sub>Br]<sup>+</sup>, 109.0/107.0 [C<sub>2</sub>H<sub>4</sub>Br]<sup>+</sup>, 78.9/80.9 [Br]<sup>+</sup>, 73.1 [C<sub>4</sub>H<sub>9</sub>O]<sup>+</sup>, 45.1 [C<sub>2</sub>H<sub>5</sub>O]<sup>+</sup>, 31.1 [CH<sub>3</sub>O]<sup>+</sup>

#### (*R*)-**2**

R<sub>f</sub> = 0.48 (petroleum ether / EtOAc) 2:1

<sup>1</sup>H-NMR: δ = 1.89 - 1.71 (d, 3 H, *J* = 6.70 Hz), 2.0 - 1.93 (m, 2 H), 3.79 - 3.75 (m, 2 H), 4.30 - 4.23 (m, 1 H) 7.20 (m, 1 H)

<sup>13</sup>C-NMR: δ = 66.90, 48.05, 43.21, 26.70

GC-MS: RT = 6.45 min, m/z [fragment] 136.0/134.0 [C<sub>4</sub>H<sub>8</sub>Br]<sup>+</sup>, 120.9/122.9 [C<sub>3</sub>H<sub>6</sub>Br]<sup>+</sup>, 109.0/107.0 [C<sub>2</sub>H<sub>4</sub>Br]<sup>+</sup>, 78.9/80.9 [Br]<sup>+</sup>, 73.1 [C<sub>4</sub>H<sub>9</sub>O]<sup>+</sup>, 45.1 [C<sub>2</sub>H<sub>5</sub>O]<sup>+</sup>, 31.1 [CH<sub>3</sub>O]<sup>+</sup>

### 3.7 Biotransformation

The biotransformation was done with lyophilized enzyme LinB starting with *rac*-dibromide **1**. The hydrolysis of the halogen atoms catalysed by the dehalogenase can proceed via to pathways going through intermediates **2** and/or **3** yielding the diol **4** shown in figure 8.

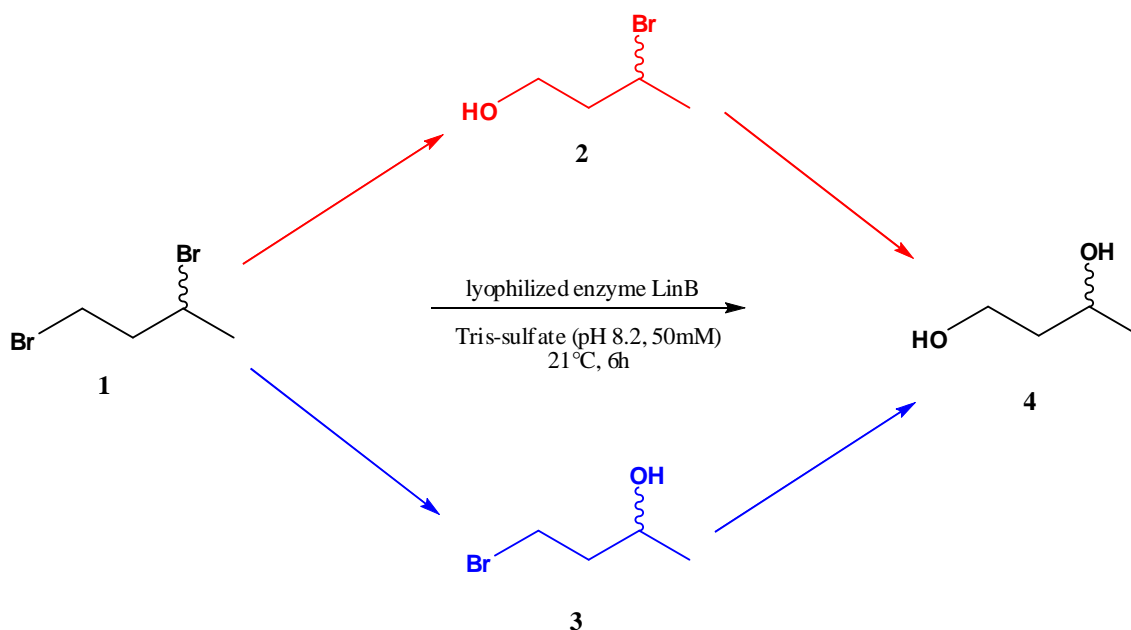


Fig. 8 Biotransformation of **1** with enzyme LinB

#### Procedure for Biotransformation

To 1 mL Tris-sulfate-buffer (pH 8.2, 50 mM) in 2 mL Eppendorf vials *rac*-1,3-dibromobutane (0.6  $\mu$ L, 5 mM) was added. Then, LinB from a stock solution (125  $\mu$ L of a 1.5 mg/mL stock solution, 187.5  $\mu$ g/mL final protein concentration) was added and the solution was incubated with shaking for 6 hours at 21 °C and 120 rpm.

The reaction was stopped by saturating the solution with NaCl and adding ethyl acetate (500  $\mu$ L). The preparation was mixed and centrifuged in an eppifuge (13000 rpm, 5 min). After second extraction, the combined organic layers were dried over NaSO<sub>4</sub> and transferred into GC-glass-vials.

### 3.8 Assignment of absolute configuration by GC

After the synthesis of the reference materials, biotransformation samples were spiked with (*R*)-2, (*S*)-2, (*R*)-3, (*S*)-3, (*R*)-4 and (*S*)-4 respectively, and analyses of the obtained GC traces allowed determination of the absolute concentration of all compounds. The results of these spiking experiments are given in figure 9 to figure 14.

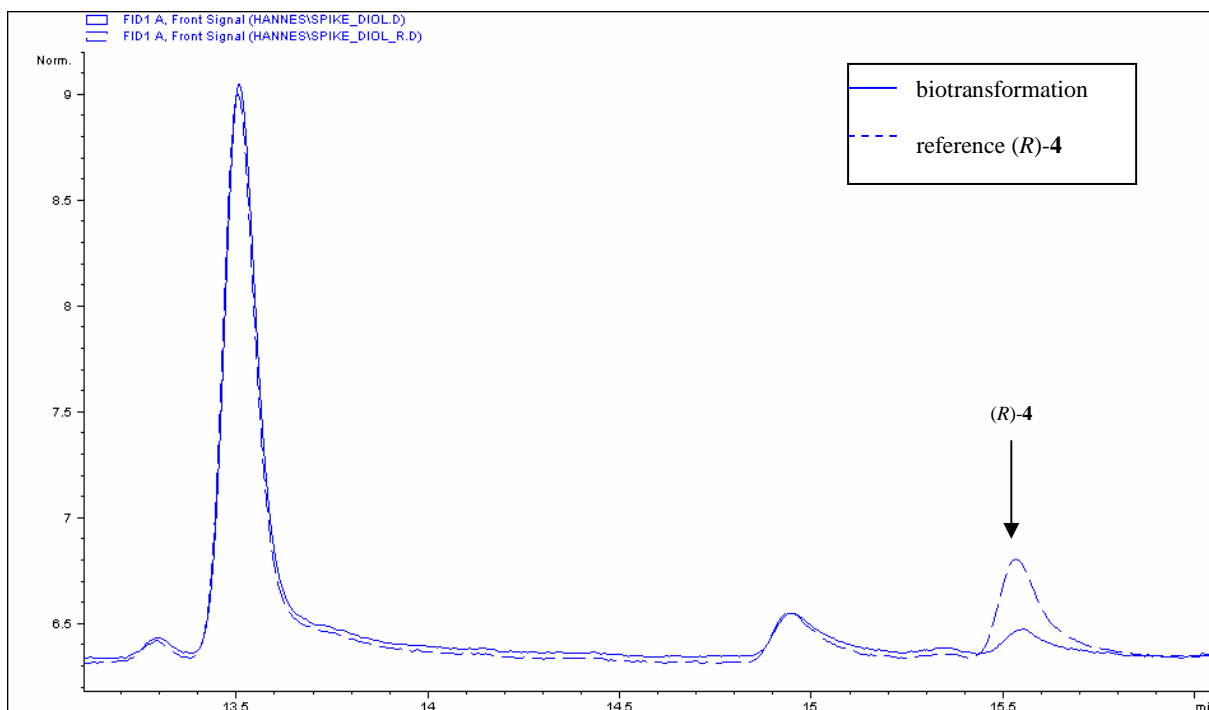


**Fig. 9** GC-FID spectra, spiking with (*R*)-4

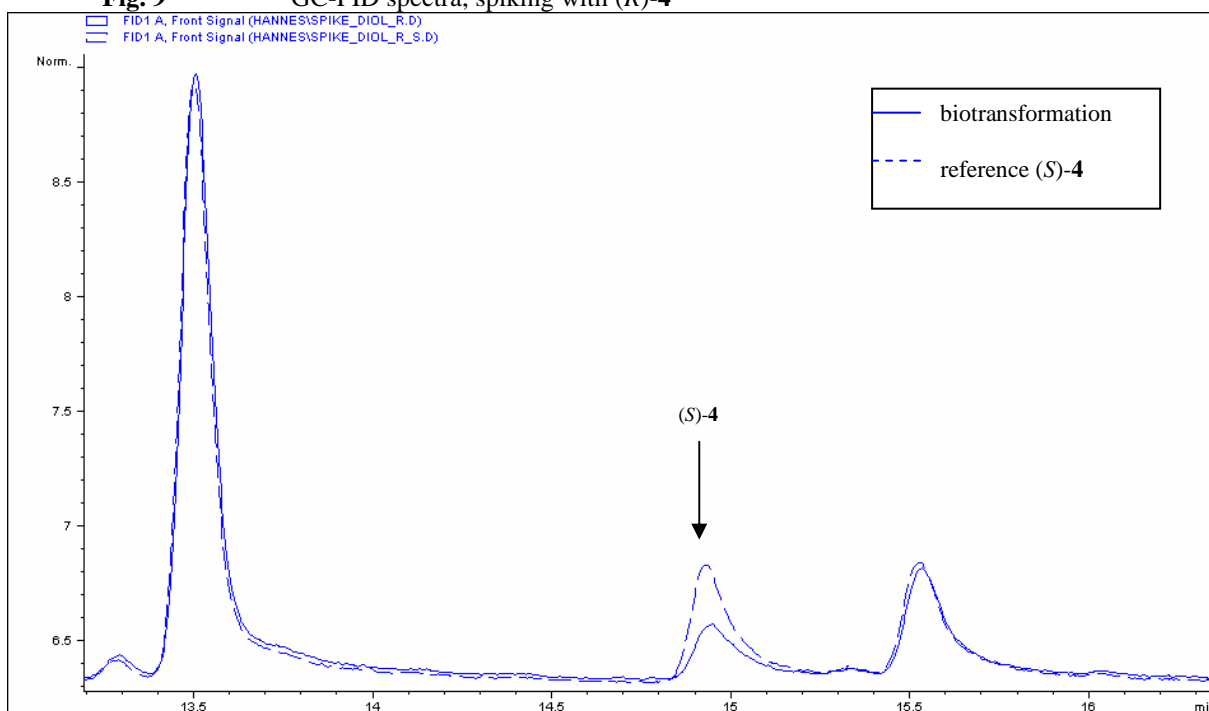


**Fig. 10** GC-FID spectra, spiking the same probe with (*S*)-4

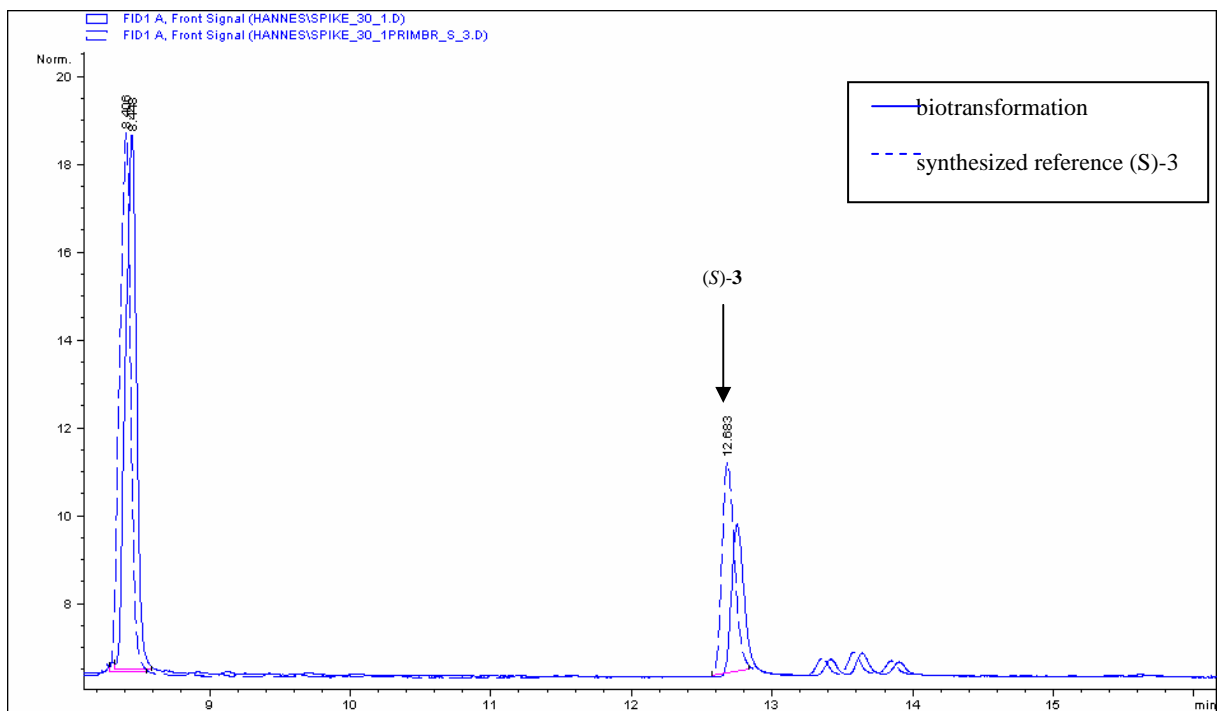


**Fig. 11** GC-FID spectra, spiking with (S)-3

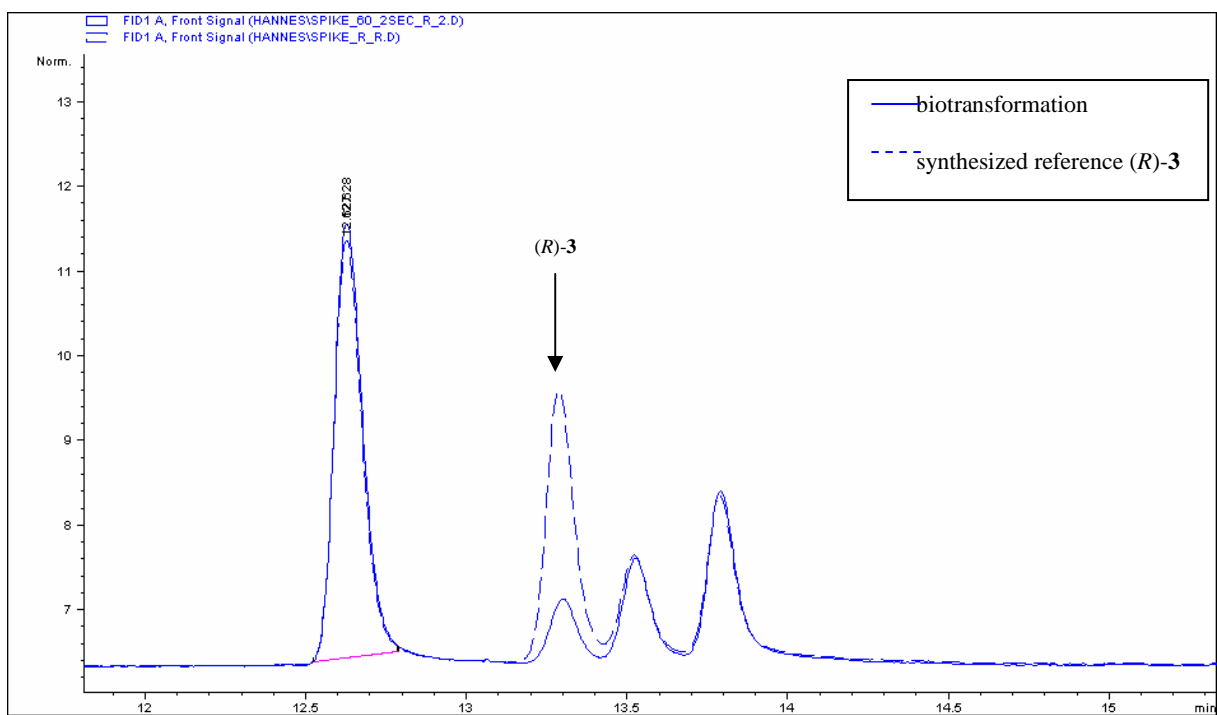


**Fig. 12** GC-FID spectra, spiking with (R)-3

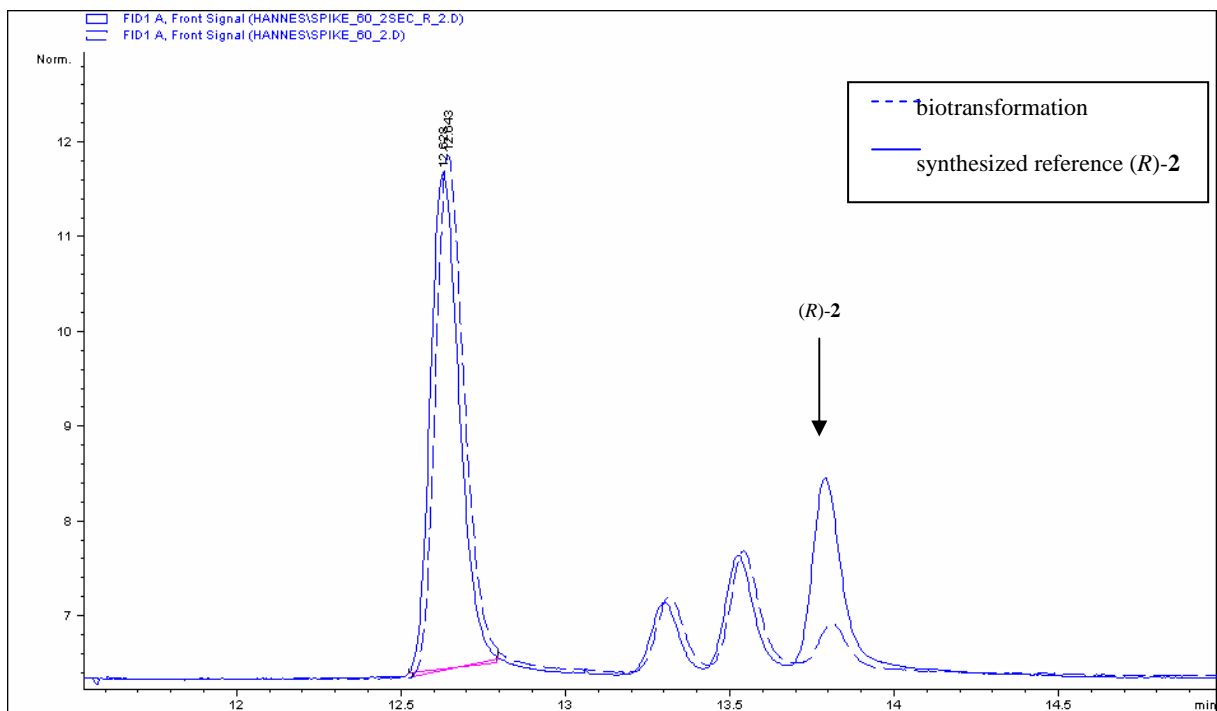


**Fig. 13** GC-FID spectra, spiking with (*R*)-2

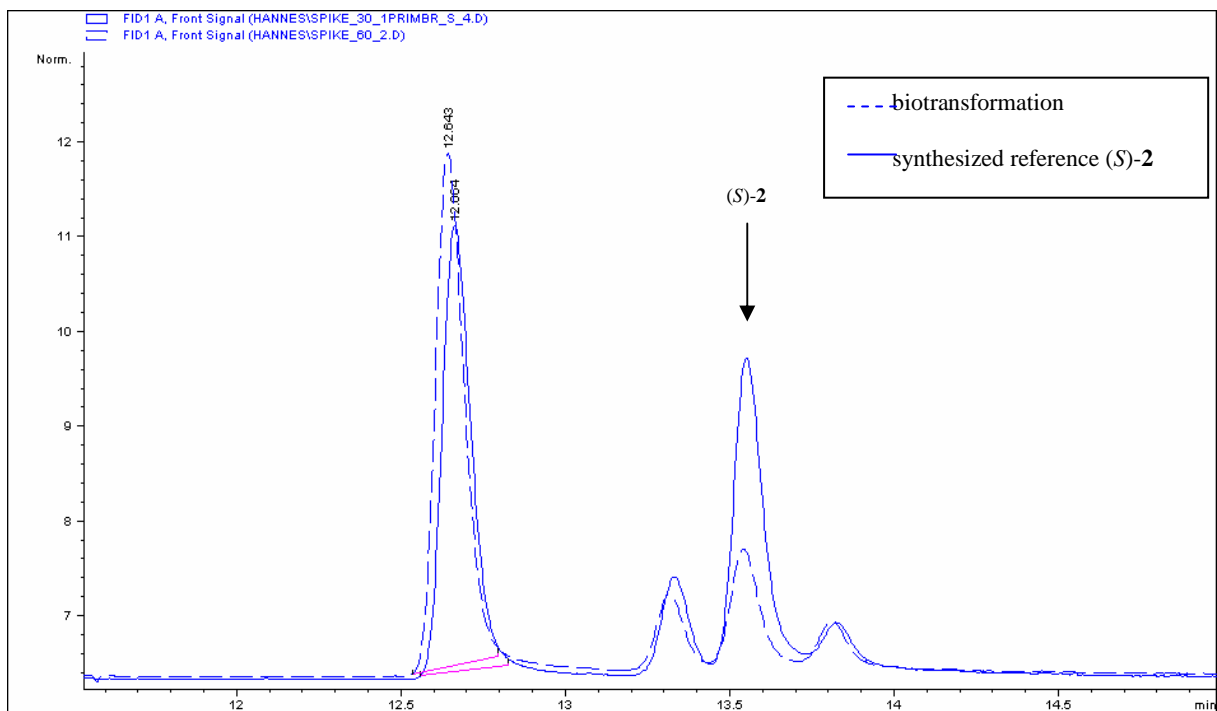


**Fig. 14** GC-FID spectra, spiking with (*S*)-2

## Conclusion

It could be shown, that for the assignment of all product peaks (except **1**) the chosen method and GC-column gave clear results. However, the peaks of the less polar dihalides (*R*)-**1** and (*S*)-**1** could not be separated.

The product peak  $R_f = 12.7$  min was identified as (*S*)-**3**,  $R_f = 13.3$  min as (*R*)-**3**,  $R_f = 13.6$  min as (*S*)-**2**,  $R_f = 13.9$  min as (*R*)-**2**,  $R_f = 14.9$  min as (*S*)-**4** and the peak at  $R_f = 15.5$  min as (*R*)-**4**. The peak with  $R_f = 8.0$  min could be assigned to the educts (*S*)-**1** and (*R*)-**1** but enantiomers were not separated. In general, for compounds **2**, **3** and **4**, (*S*)-enantiomers are eluting first. All results are summarized in table 4.

### 3.9. Kinetic Resolution of 1,3-Dibromobutane with LinB

For getting access to kinetic data, a time study was done. Herein samples were taken after 10, 30, 60, 90 and 120 minutes. Analytical data shown in figure 15 represent the amount of **1**, **2**, **3** and **4** at specific time points. Due to the high polarity of diol **4**, leading to incomplete recovery from the aqueous phase by extraction, its amount could not be accurately measured, but was calculated as the difference of all compounds to 100 %.

In order to compensate for the different GC response factors of the reference compounds, calibration curves were prepared as shown in figure 7.

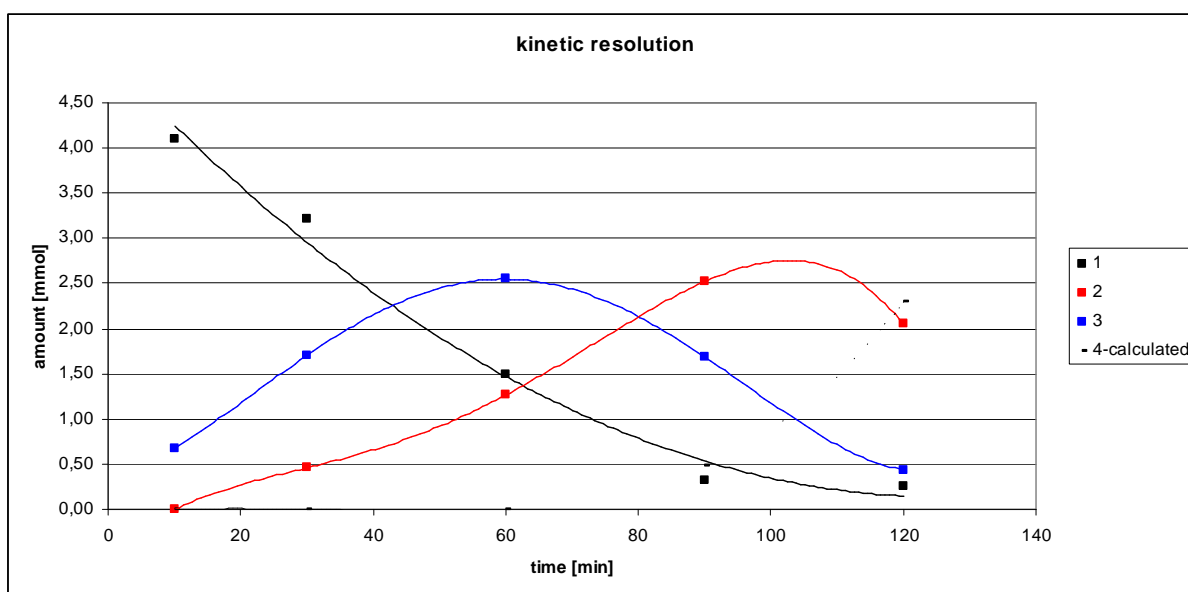
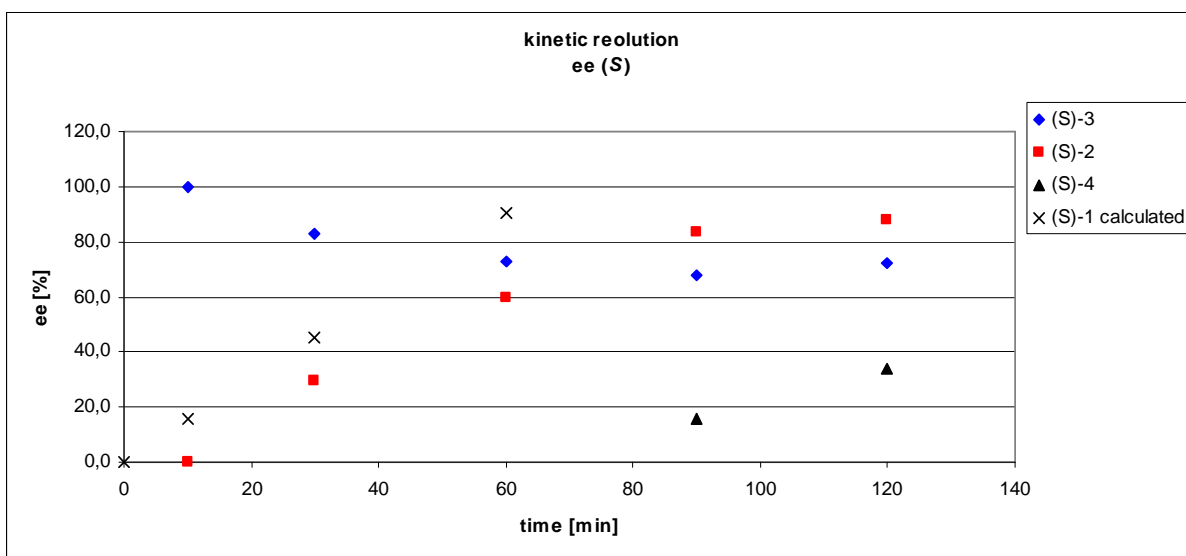


Fig. 15 Time study of LinB-catalysed hydrolysis of *rac*-**1**



**Fig. 16** Ee-values of (S)-2, (S)-3 and (S)-4 over time

The ee-values of the intermediates (S)-2, (S)-3 and of product (S)-4 are given in figure 16. The ee-value of (S)-3, after the first 10 min at high values (>99%), remains rather stable over time and persists at modest 80 %. The ee-value of the product (S)-4 could only be detected after 90 minutes where the calculated amount was higher than 50 %. Here it is shown that the ee-value increases from low 20 % to finally low 40%. Due to the analytical separation problem of the educts (S)-1 and (R)-1, those values could not be given in figure 16.

## Reaction Rate and Kinetic Coefficient k

The kinetic coefficient k is defined as the change of concentration over time given in formula 1. Here, the coefficient k was calculated with data from the time study and represents the velocity of intermediate / product formation of (S)-2, (R)-2, (S)-3, (R)-3 and (S)-4 in the unit of [mM/min]. The results and k-values are shown in figure 19 - figure 22. Herein, for each enantiomer the k-values between 0-10 minutes (where possible), 10-30 minutes, 30-60 minutes, 60-90 minutes and 90-120 minutes were calculated.

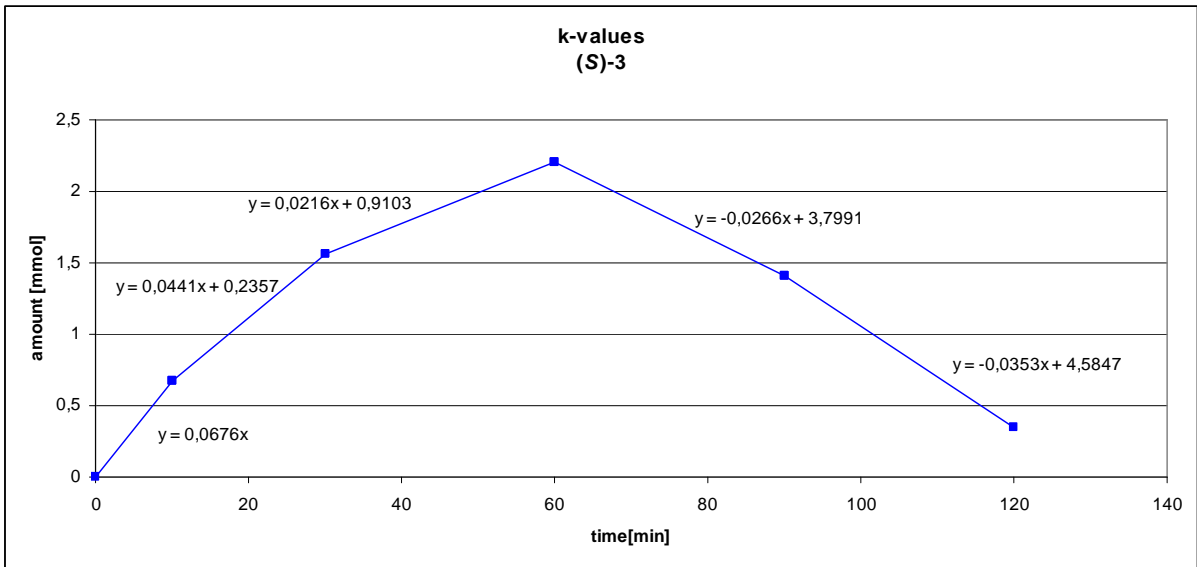


**Fig. 17** Calculation of k-values for (S)-3

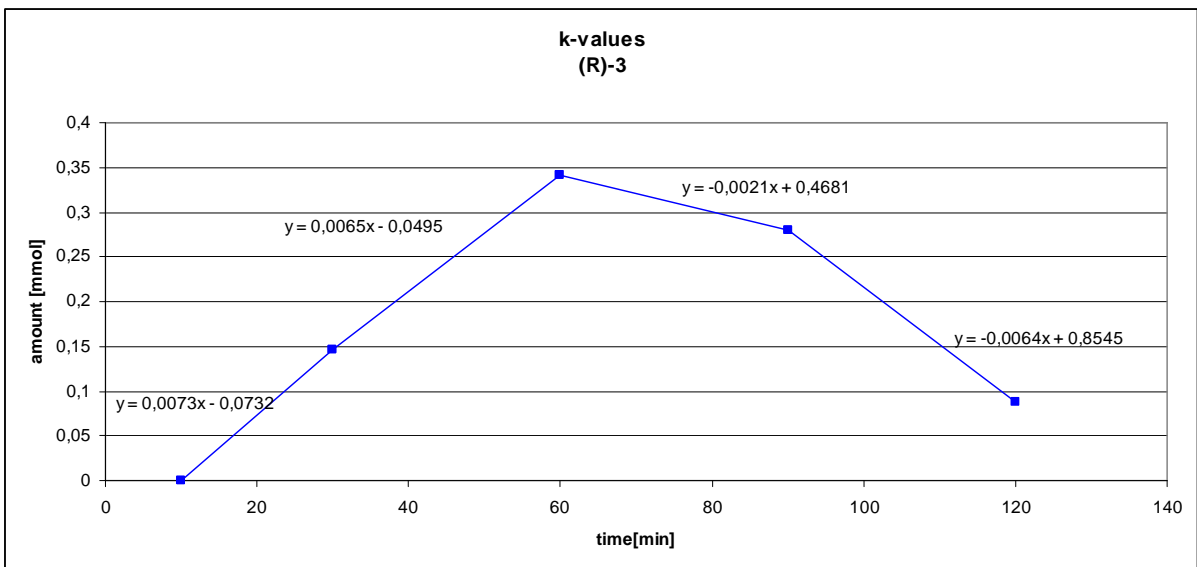


**Fig. 18** Calculation of k-values for (R)-3

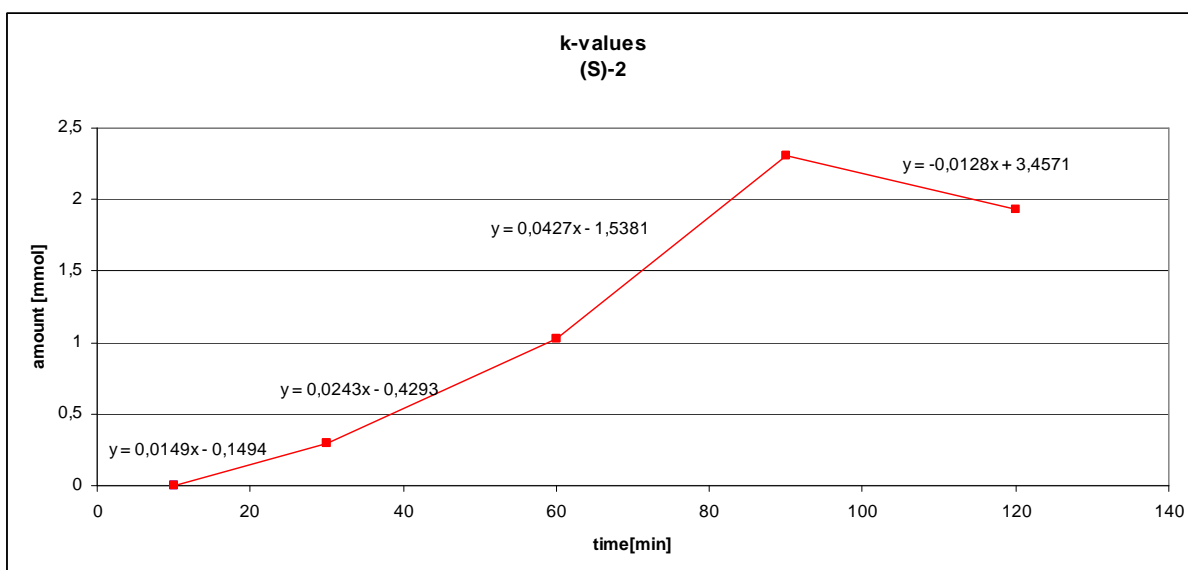


**Fig. 19** Calculation of k-values for (S)-2

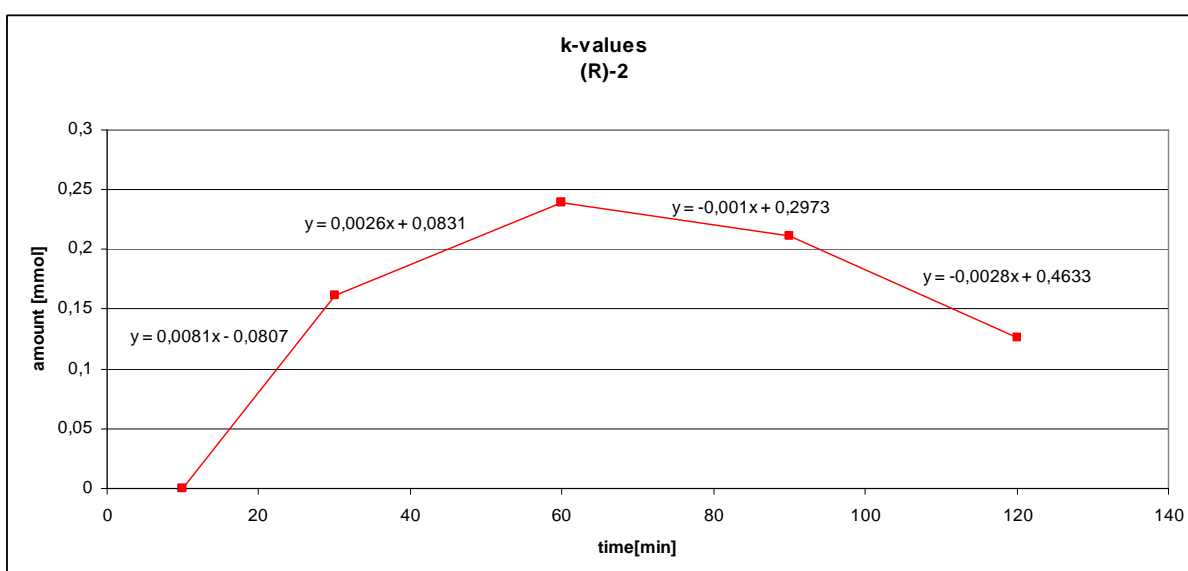


**Fig. 20** Calculation of k-values for (R)-2

For a better overview, the k-values of (S)-3 and (R)-2, which have the same educt (R)-1, and the k-values of (S)-2 and (R)-3 which have (S)-1 as educt were plotted against the reaction time. This correlation is given in figure 21 and figure 22.

As shown in figure 21, the k-values of (S)-3 and (R)-2 are decreasing and staying positive from the beginning until approximately 70 minutes. This fact could be interpreted, taking into account that the higher the educt concentration (R)-1, the higher the k-value. Up to this point, the velocity of intermediate formation is higher than the second dehalogenation step yielding (S)-4. After ~70 minutes, the k-value increases in negative direction which means, that the velocity of product formation to (S)-4 becomes the dominant process.

The k-values of (S)-2 and (R)-3 are showing a different behaviour (figure 22). Here the k-value of (S)-2 is increasing with time and the velocity of intermediate formation reaches its maximum after 90 minutes. At this point, the k-value of (R)-3 is already negative which means, that the product formation to (R)-4 is already ongoing and faster than the product formation starting from (S)-2. The results of all k-values are summarized in table 5.

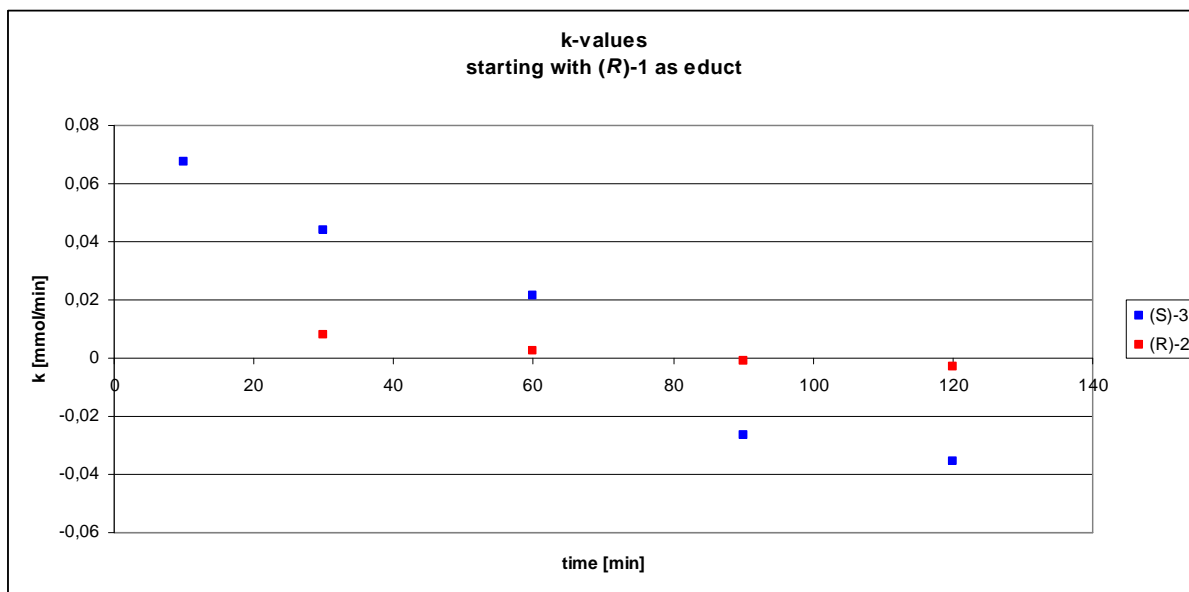


**Fig. 21** Calculated k-values for (S)-3 and (R)-2 between intermediate time points

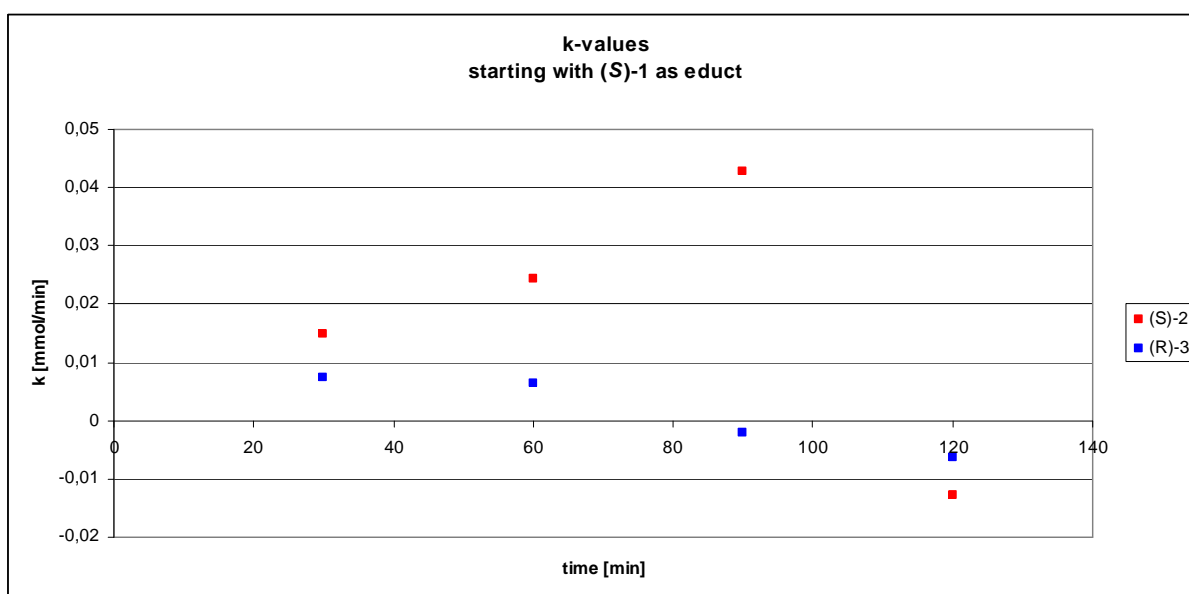


**Fig. 22** Calculated k-values for (S)-2 and (R)-3 between intermediate time points

With the e.e. value of (S)-**4** and (R)-**4** as well as the calculated concentration of **4**, the k-values for the diol could be calculated between 90 and 120 minutes. Those results are given in figure 25. The velocity of product (S)-**4** formation is much faster than formation of (R)-**4** at that particular time.

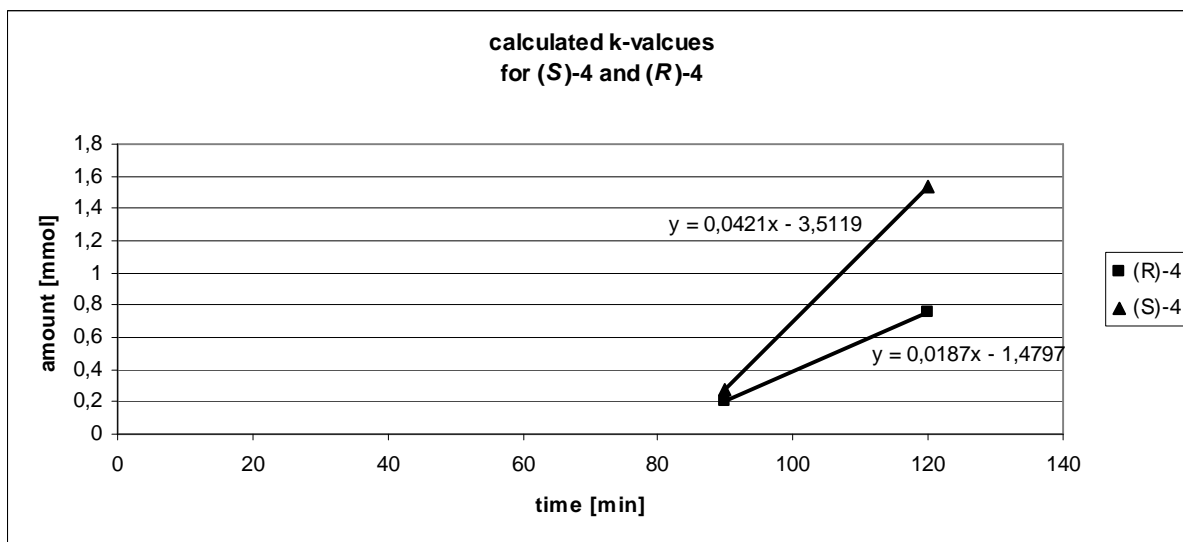


Fig. 23 Calculated k-values for (S)-**4** and (R)-**4**

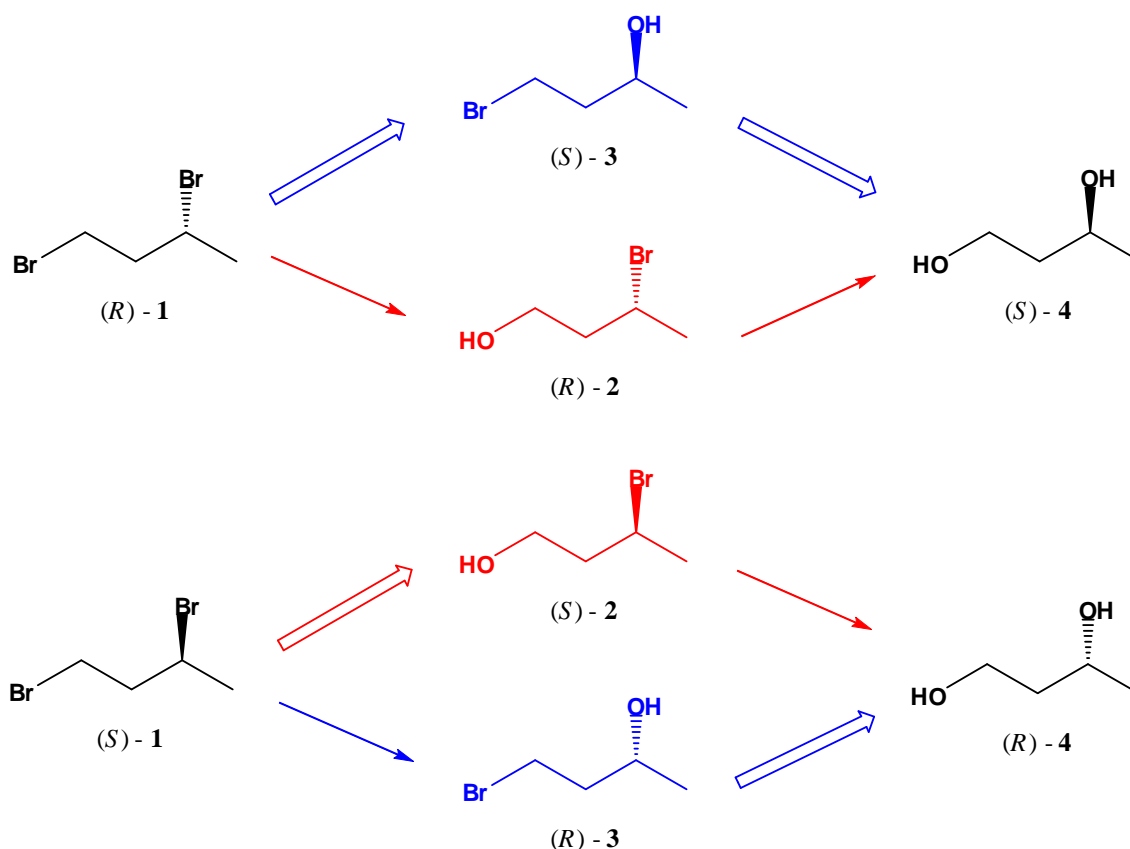
Actually, the k-value of (S)-**4** has to be seen as a sum of (S)-**3** and (R)-**2** as educts and the k-value of (R)-**4** as a sum of (S)-**2** and (R)-**3** as educts.

Table 5 k-Values of all intermediates and products

time [min]	k-value (S)-3 [mmol/min]	k-value (R)-2 [mmol/min]	k-value (S)-2 [mmol/min]	k-value (R)-3 [mmol/min]	k-value (S)-2 [mmol/min]	k-value (R)-4 [mmol/min]
0 to 10	0,0676					
10 to 30	0,0441	0,0081	0,0149	0,0073		
30 to 60	0,0216	0,0026	0,0243	0,0065		
60 to 90	-0,0266	-0,001	0,0427	-0,0021		
90 to 120	-0,0353	-0,0028	-0,0128	-0,0064	0,0421	0,0019

## Conclusion

For both intermediates **2** and **3**, the reaction rate of the (*S*)-configuration is up to ~5 times higher than that of the (*R*)-configuration. The *k*-values of (*S*)-**2** and (*S*)-**3** are in same range but the *k*-value of (*S*)-**3** is a little higher. This conclusion is congruent to figure 15. Here, the amount of **3** at 60 minutes is nearly twice as much as the amount of **2**. This means that up to 60 minutes the formation of **3** is faster than the subsequent reaction to **4**, thus allowing accumulation of **3** before further conversion. The formation of **2** has a time offset and up to 90 minutes the formation of intermediate **2** is faster than the forward reaction.



**Scheme 20** Relative velocity of individual steps in the dehalogenation of (*R*)- and (*S*)-**1**.

Scheme 20 shows the possible reaction routes going from **1** to **4**. As discussed above, the *k*-values are changing over the time but their order of magnitude can be summarized in that way. The bigger arrows symbolize faster routes and are congruent to the prediction of figure 8.

## References

- [1] G.W. Gribble *Chemosphere*, **2003**, *52*, 289-97
- [2] „*Toxikologie: Band 2 - Toxikologie der Stoffe*“, Hans-Werner Vohr, **2012**, Wiley-VCH
- [3] Dissertation "*Leichtflüchtige halogeniert Kohlenwasserstoffe - Vorkommen, Verhalten und Bedeutung in Küstengebieten*", O. Christof, Universität Hamburg, **2012**
- [4] „*Organische Chemie*“, K. Peter, C. Vollhard, N. E. Schore, **2005**, Wiley-VCH, 4. Auflage, pp. 239-240
- [5] "*Biotransformations in organic chemistry*", K. Faber, 6th Edition, **2011**, Springer, pp. 257-264
- [6] K.-H. van Pèe, S. Unversucht, *Chemosphere*, **2003**, *52*, 299-312
- [7] D. B. Janssen, J. E. Oppentocht, G. J. Poelarends, *Curr. Opin. Biotechnol.*, **2001**, *12*, 254-258
- [8] Y. Nagata, Z. Prokop, Y. Sato, P. Jerabek, A. Kumar, Y. Ohtsubo, M. Tsuda, J. Damborsky, *Appl. Environ. Microbiol.*, **2005**, *71* (4), 2183-2185
- [9] V. A. Streltsov, Z. Prokop, J. Damborsky, Y. Nagata, A. Oakley, M. C. J. Wilce, *Biochemistry*, **2003**, *42*, 10104-10112
- [10] A. J. Oakley, Z. Prokop, M. Bohac, J. Kmunicek, T. Jedlicka, M. Monincova, I. Kuta- Smatanova, Y. Nagata, J. Damborsky, M. C.J. Wilce, *Biochemistry*, **2002**, *41*, 4847-4855
- [11] Z. Prokop, M. Monincova, R. Chaloupkova, M. Klvana, Y. Nagata, D. B. Janssen, J. Damborsky, *J. Biol. Chem.*, **2003**, *278* (46), 45094-45100
- [12] J. Tercio, B. Ferreira, F. Simonelli, *Tetrahedron*, **1990**, *46* (18), 6311-6318
- [13] Y. Nakamura, K. Mori, *Eur. J. Org. Chem.* **1999**, 42175-2182
- [14] T. W. Baughman, J. C. Sworen, K. B. Wagener, *Tetrahedron*, **2004**, *60*, 10943-10948
- [15] I. Uemura, K. Yamda, K. Sugiura, H. Miyagawa, T. Ueno, *Tetrahedron*, **2001**, *12*, 943-947
- [16] M. Schober, K. Faber, *Trends Biotechnol.* **2013**, *31*, 468-478
- [17] UNIDO, United Nations Industrial Development Organization;  
<http://www.unido.org/index.php?id=5167>; 23.01.2015
- [18] Y. Nagata, K. Miyauchi, J. Damborsky, K. Manova, A. Ansorgova, M. Takagi, *Appl. Environ. Microbiol.* **1997**, *63*, 3707-3710

## Abbreviations

1,2-DCE	1,2-dichloroethane
1,2-DCP	1,2-dichloropropane
AcOH	acetic acid
BP	boiling point
DDT	dichlordiphenyltrichlorethane
DMAP	4-(dimethylamino)-pyridine
DMF	dimethyl formamide
ee	enantiomeric excess
EtOAc	ethyl acetate
FCCH	flouro-chloro-hydrocarbon
FID	flame ionization detector
GC	gas chromatography
HCH	hexachlorocyclohexane
MS	mass spectrum
m/z	mass per charge
n.d.	not determined
NMR	nuclear magnetic resonance
PCB	polychlorinated biphenyls
ppm	parts per million
<i>rac</i>	racemic
R <sub>f</sub>	retention factor
rpm	rotation per minute
RT	room temperature
THF	tetrahydrofuran
TLC	thin layer chromatography
TMS	tetramethyl silane
Tris	Tris(hydroxymethyl)-aminomethane
trityl chloride	Triphenylchloromethane

## Publications

J. Gross, K. Tauber, M. Fuchs, N. G. Schmidt, A. Rajagopalan, K. Faber, W. M. F. Fabian, J. Pfeffer, T. Haas and W. Kroutil, *Green Chem.*, **2014**, *16*, 2117–2121

C. Wuensch, J. Gross, G. Steinkellner, A. Lyskowski, K. Gruber, S. M. Glueck and K. Faber, *RSC Adv.*, **2014**, *4*, 9673–9679

C. Wuensch, N. Schmidt, J. Grossa, B. Grischek, S. M. Glueck, K. Faber, *J. Biotechnol.*, **2013**, *168*, 264–270

C. Wuensch, J. Gross, G. Steinkellner, K. Gruber, S. M. Glueck, and K. Faber, *Angew. Chem. Int. Ed.*, **2013**, *52*, 2293-2297

C. Wuensch, S. M. Glueck, J. Gross, D. Koszelewski, M. Schober, and K. Faber, *Org. Lett.*, **2012**, *14*, 1974–1977

D. Clay, D. Koszelewski, B. Grischek, J. Gross, I. Lavandera, W. Kroutil, *Tetrahedron*, **2010**, *21*, 2005-2009

I. Lavandera, G. Oberdorfer, J. Gross, S. de Wildeman, W. Kroutil, *Eur. J. Org. Chem.*, **2008**, 2539-2543

I. Lavandera, A. Kern, M. Schaffenberger, J. Gross, A. Glieder, S. de Wildeman, W. Kroutil, *ChemSusChem*, **2008**, *1*, 461-436

H. Mang, J. Gross, M. Lara, C. Goessler, H. E. Schoemaker, G. M. Guebitz, W. Kroutil, *Tetrahedron*, **2007**, *63*, 3350-3354

C. Gruber, B. M. Nestl, J. Gross, P. Hildebrandt, U. T. Bornscheuer, K. Faber, W. Kroutil, *Chem. Eur. J.*, **2007**, *13*, 8271-8276

K. Edegger, H. Mang, K. Faber, J. Gross, *J. Mol. Catal. A. Chem.*, **2006**, *251*, 66-70

H. Mang, J. Gross, M. Lara, C. Goessler, H. E. Schoemaker, G. M. Guebitz, W. Kroutil, *Angew. Chem. Int. Ed.*, **2006**, *45*, 5201-5203

## Supplementary data

File :C:\msdchem\1\data\Hannes\14-04-23\HG\_5.D  
Operator : hannes  
Acquired : 23 Apr 2014 10:32 using AcqMethod ACHIRAL-MSD\_LOWBOILERS.M  
Instrument : 5975  
Sample Name: HG 5  
Misc Info :  
Vial Number: 16

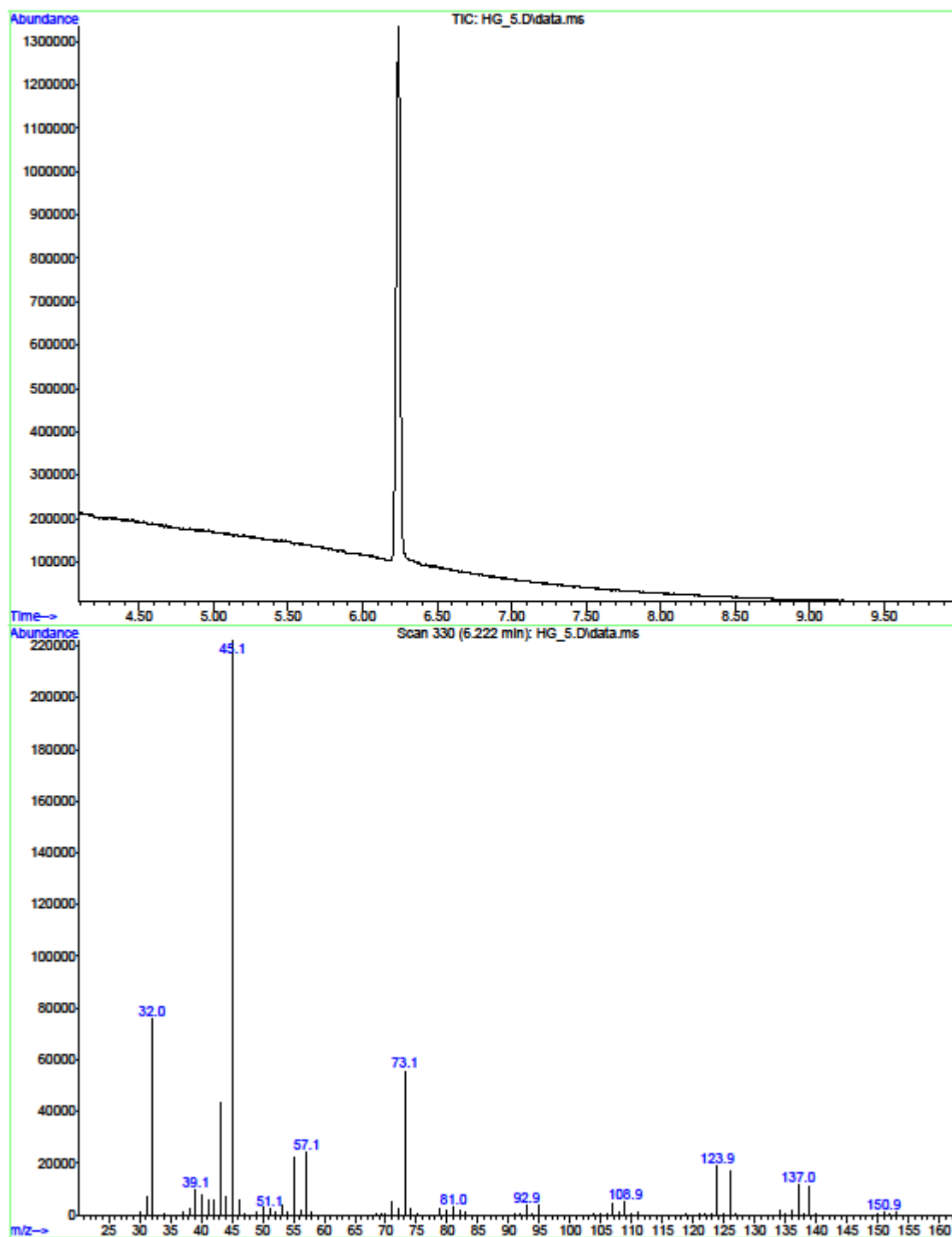
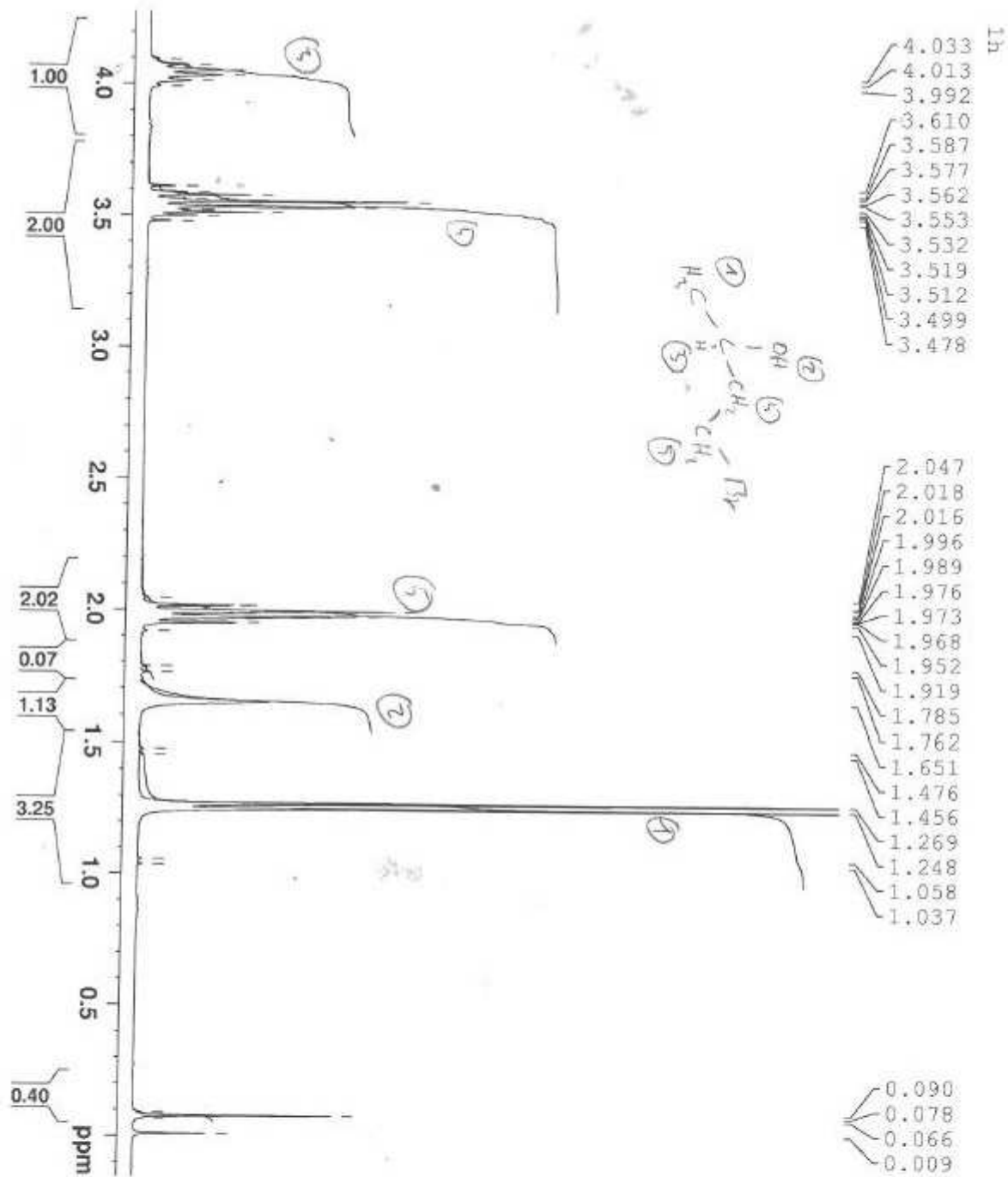


Figure 24 GC-MS spectrum of (*R*)-3



**BRUKER**

NAME: WC\_JC\_X04  
 EXPNO: 10  
 PROCNO: 1  
 Date\_: 20140429  
 Time: 17.48  
 INSTRUM: spect  
 PROBRD: 5 mm PABBO 93-  
 PULPROG: zg30  
 ID: 49504  
 SOLVENT: CDCl3  
 NS: 16  
 DS: 2  
 SWH: 6188.119 Hz  
 FIDRES: 0.1155002 Hz  
 AQ: 3.9999731 sec  
 RG: 64  
 DW: 80.800 usec  
 DE: 6.30 usec  
 TE: 295.8 K  
 D1: 1.00000000 sec  
 ID0: 1

CHANNEL f1 -----  
 NU01: 1H  
 P1: 10.50 usec  
 PL1: 0.00 dB  
 P1LW: 12.584458086 W  
 SFO1: 300.1318534 MHz  
 SI: 32766  
 SF: 300.1350000 MHz  
 WDW: EM  
 SSB: 0  
 LB: 0.30 Hz  
 GB: 0  
 PC: 1.00

Figure 25 <sup>1</sup>H-NMR spectrum of (R)-3



File :C:\msdchem\1\data\Hannes\14-04-16\HG\_syn\_Br\_low.D  
Operator : tamara  
Acquired : 16 Apr 2014 23:59 using AcqMethod ACHIRAL-MSD\_LOWBOILERS.M  
Instrument : 5975  
Sample Name: HG syn Br low  
Misc Info :  
Vial Number: 81

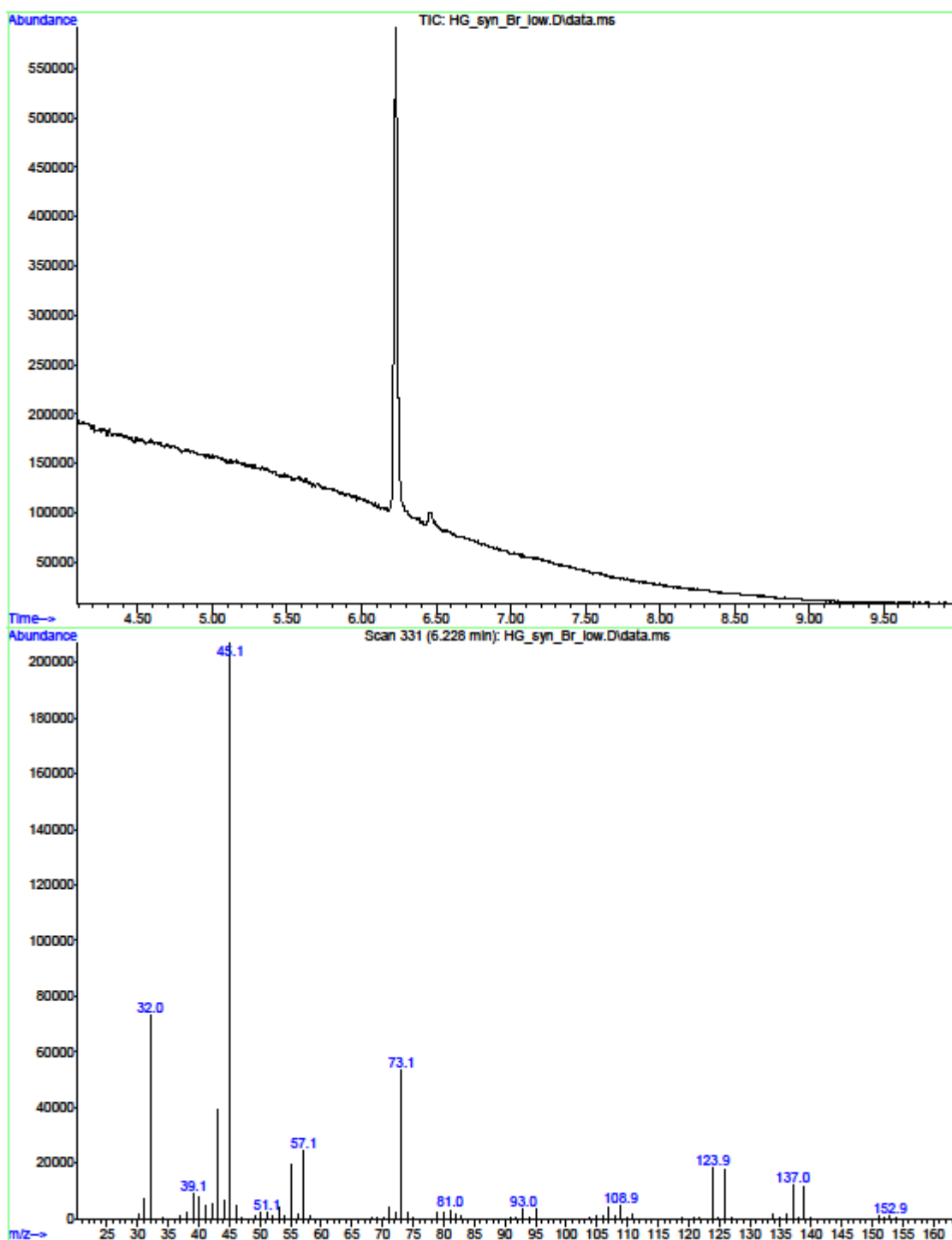
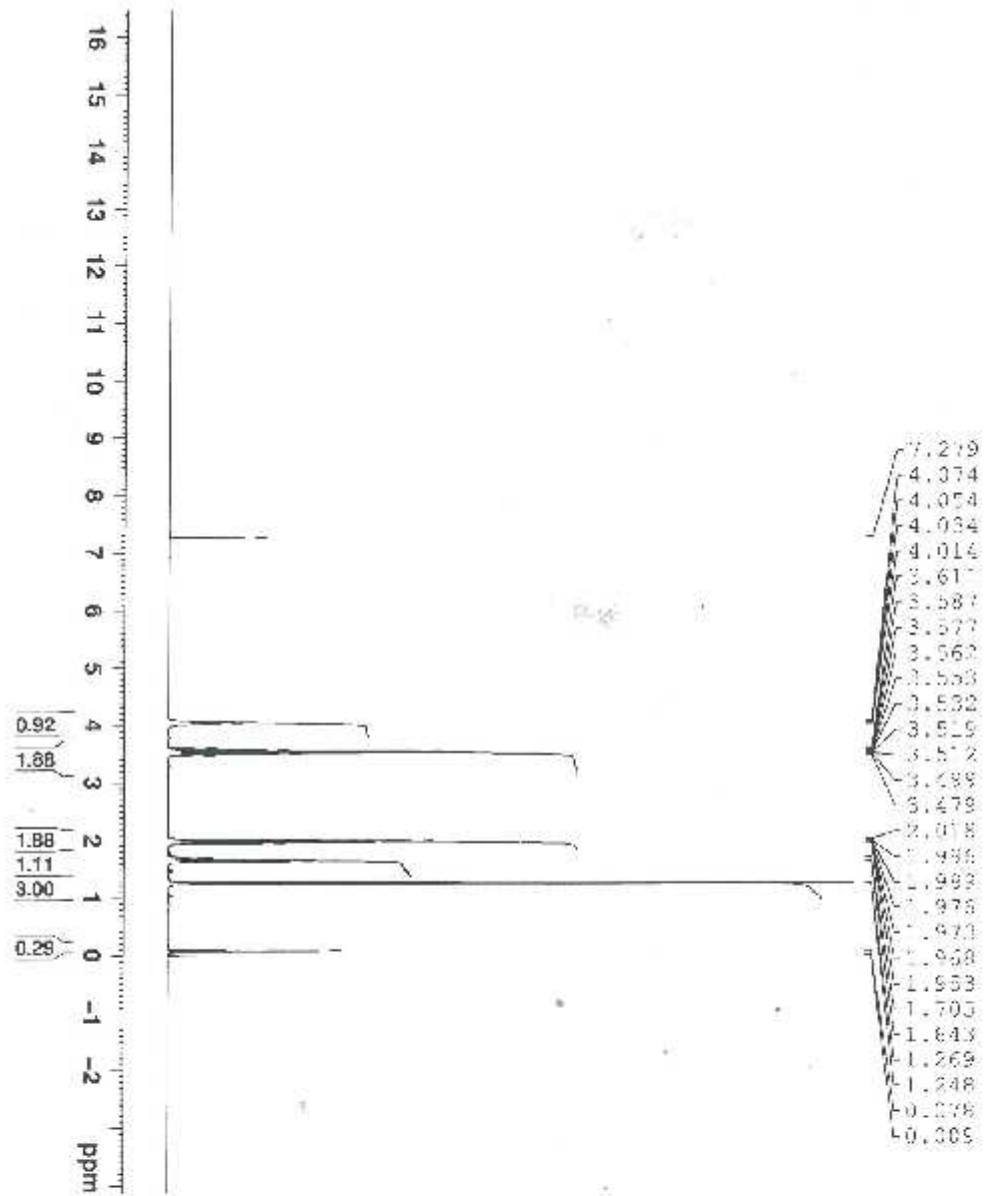


Figure 27 GC-MS spectrum of (S)-3

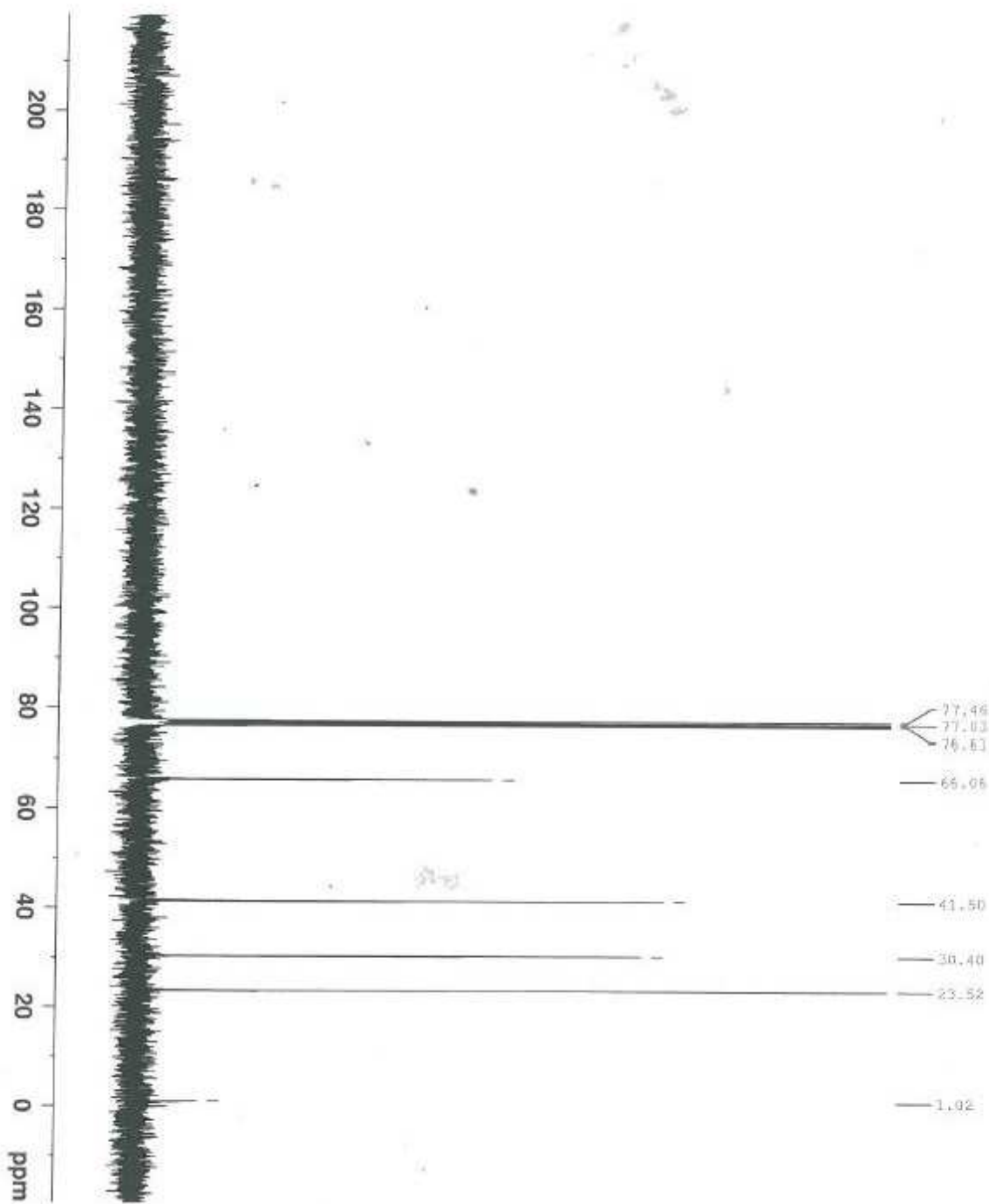


**BRUKER**

NAME: 411-70-7-48  
 DATE: 2017-12-23  
 TIME: 12:49  
 PULPROG: zgpg30  
 PROCNO: 1  
 F2: 500.136  
 F1: 500.136  
 AQ: 1.00  
 SI: 32768  
 SF: 500.136  
 DS: 4  
 AS: 0  
 LA: 0  
 GB: 0  
 PC: 1  
 TD: 1  
 DE: 6.50  
 TE: 297.2  
 D1: 1.00000000  
 T1: 1.00000000  
 T2: 1.00000000  
 T3: 1.00000000  
 T4: 1.00000000  
 T5: 1.00000000  
 T6: 1.00000000  
 T7: 1.00000000  
 T8: 1.00000000  
 T9: 1.00000000  
 T10: 1.00000000  
 T11: 1.00000000  
 T12: 1.00000000  
 T13: 1.00000000  
 T14: 1.00000000  
 T15: 1.00000000  
 T16: 1.00000000  
 T17: 1.00000000  
 T18: 1.00000000  
 T19: 1.00000000  
 T20: 1.00000000

NAME: 411-70-7-48  
 DATE: 2017-12-23  
 TIME: 12:49  
 PULPROG: zgpg30  
 PROCNO: 1  
 F2: 500.136  
 F1: 500.136  
 AQ: 1.00  
 SI: 32768  
 SF: 500.136  
 DS: 4  
 AS: 0  
 LA: 0  
 GB: 0  
 PC: 1  
 TD: 1  
 DE: 6.50  
 TE: 297.2  
 D1: 1.00000000  
 T1: 1.00000000  
 T2: 1.00000000  
 T3: 1.00000000  
 T4: 1.00000000  
 T5: 1.00000000  
 T6: 1.00000000  
 T7: 1.00000000  
 T8: 1.00000000  
 T9: 1.00000000  
 T10: 1.00000000  
 T11: 1.00000000  
 T12: 1.00000000  
 T13: 1.00000000  
 T14: 1.00000000  
 T15: 1.00000000  
 T16: 1.00000000  
 T17: 1.00000000  
 T18: 1.00000000  
 T19: 1.00000000  
 T20: 1.00000000

Figure 28 <sup>1</sup>H-NMR spectrum of (S)-3



```

NAME          wd_jc_3-bf
EXPNO         11
PROCNO        1
Date_         20140423
Time          14.16
INSTRUM       spect
PROBHD        5 mm F4BBO BB-
PULPROG       zgpg30
TD            65536
SOLVENT       CDCl3
NS            812
DS            4
SWH           18028.946 Hz
FIDRES        0.500051 Hz
AQ            0.9999476 sec
RG            2050
OR            27.733 usec
DE            6.50 usec
TE            296.2 K
D1            2.00000000 sec
D11           0.09000000 sec
TD0           1

===== CHANNEL #1 =====
NUC1          13C
P1            10.50 usec
PL1           0.00 dB
PL1W          40.19018173 W
SFO1          75.4752953 MHz

===== CHANNEL #2 =====
CPDPRG2      waltz16
NUC2          1H
PCPD2        90.00 usec
PL2           0.00 dB
PL2W         20.00 dB
PL3           20.00 dB
PL3W         12.58459086 W
PL4W         0.12574957 W
PL5W         0.112584551 W
SFO2         300.1312005 MHz
SI            32769
SF           75.4677490 MHz
WDW           EM
SSB           0
LB            1.00 Hz
GB            0
PC            1.40
    
```

Figure 29 <sup>13</sup>C-NMR spectrum of (S)-3

File :C:\msdchem\1\data\Hannes\14-06-30\HG\_lastsyn\_low.D  
Operator : hannes  
Acquired : 30 Jun 2014 16:02 using AcqMethod ACHIRAL-MSD\_LOWBOILERS.M  
Instrument : 5975  
Sample Name: HG lastsyn low  
Misc Info :  
Vial Number: 29

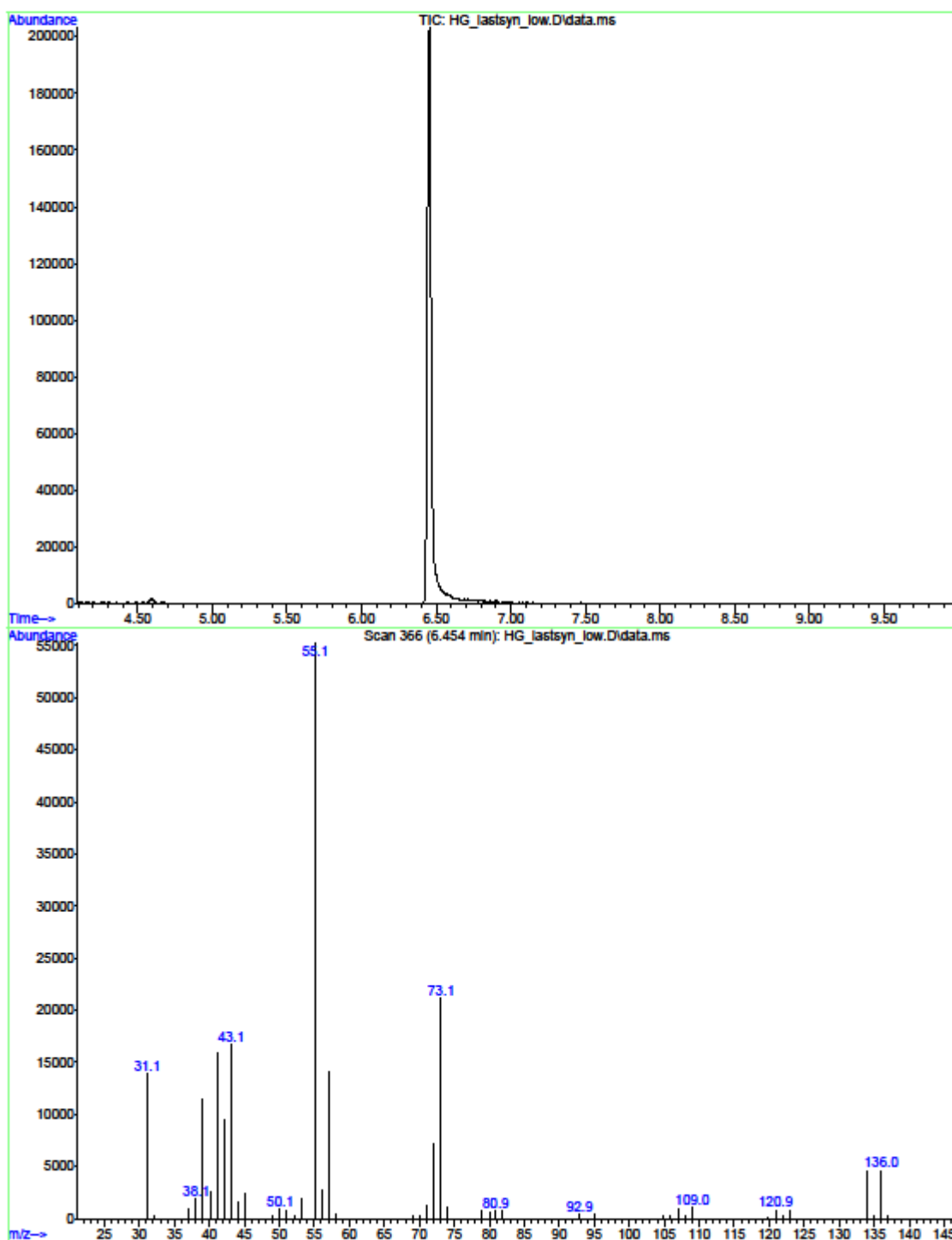


Figure 30 GC-MS spectrum of (R)-2



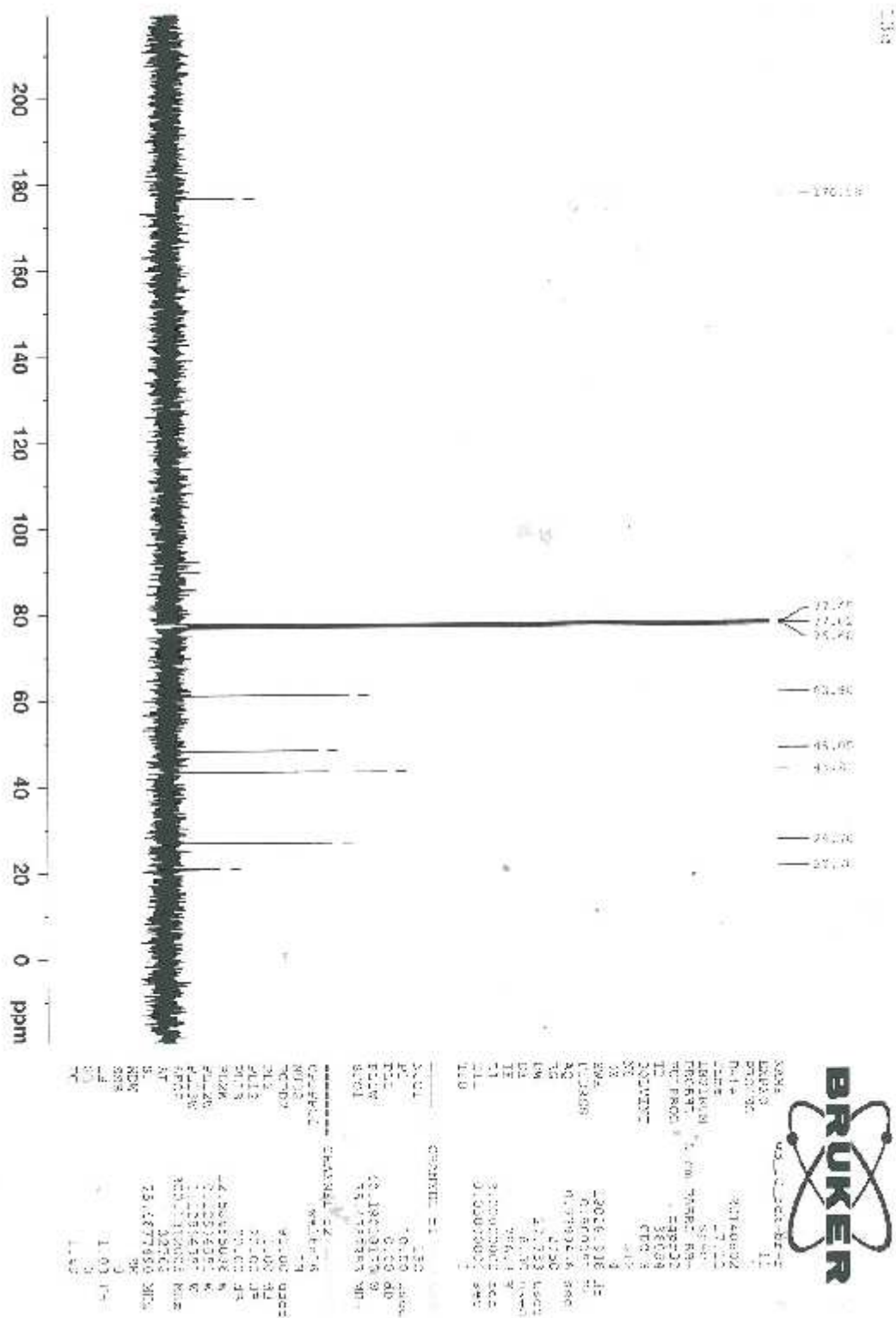


Figure 32 <sup>13</sup>C-NMR spectrum of (R)-2

File :C:\msdchem\1\data\Hannes\14-06-02\_2\HG\_Fr7\_14\_low.D  
Operator : joerq  
Acquired : 2 Jun 2014 19:01 using AcqMethod ACHIRAL-MSD\_LOWBOILERS.M  
Instrument : 5975  
Sample Name: HG Fr7 14 low  
Misc Info :  
Vial Number: 21

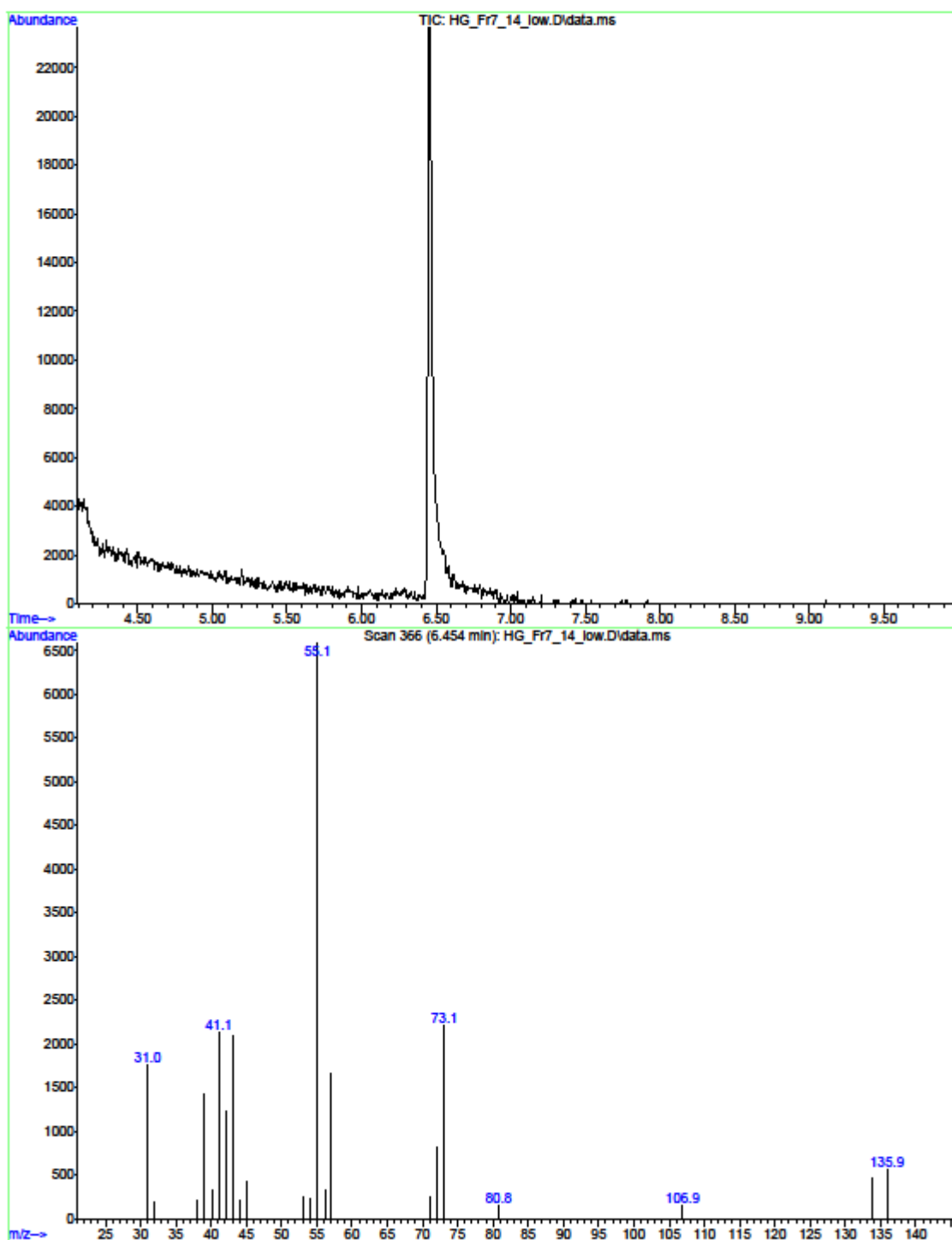


Figure 33 GC-MS spectrum of (S)-2

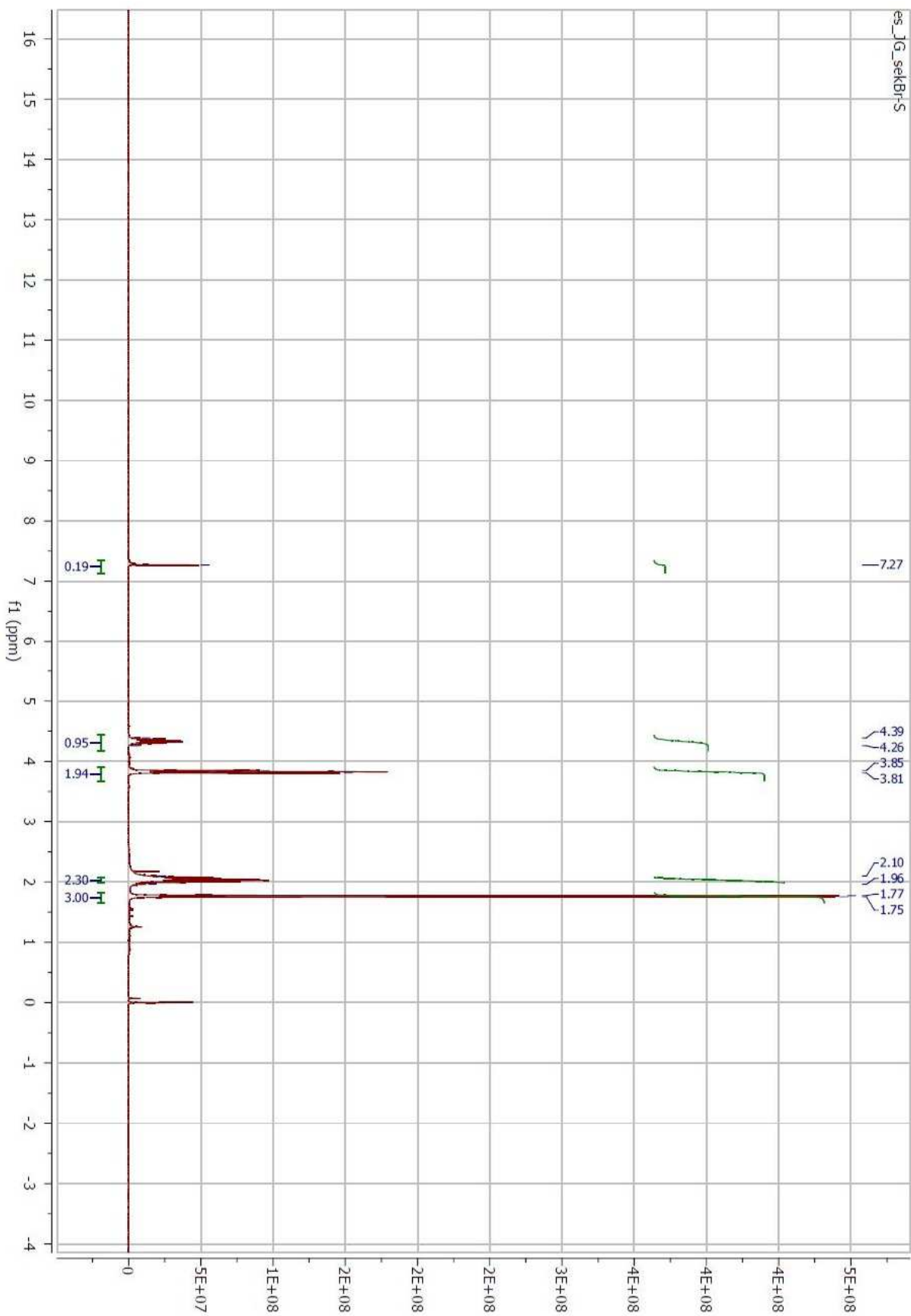


Figure 34  $^1\text{H}$ -NMR spectrum of (S)-2

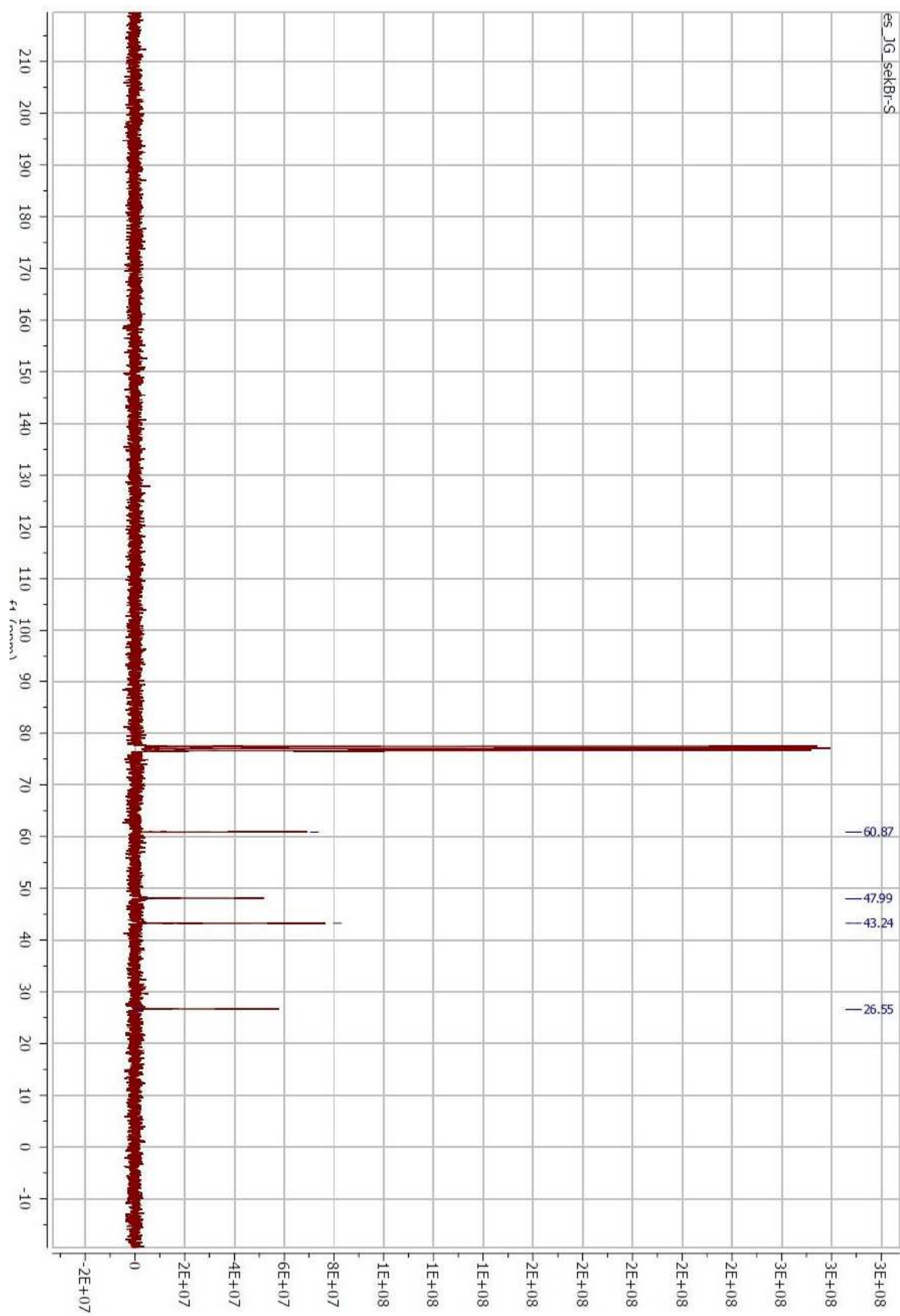


Figure 35  $^{13}\text{C}$ -NMR spectrum of (S)-2

File : C:\msdchem\1\data\Hannes\14-03-28-syn\HG\_synTs\_R.D  
Operator : Niki  
Acquired : 27 Mar 2014 14:17 using AcqMethod ACHIRAL-MSD.M  
Instrument : 5975  
Sample Name: HG\_synTs R  
Misc Info :  
Vial Number: 93

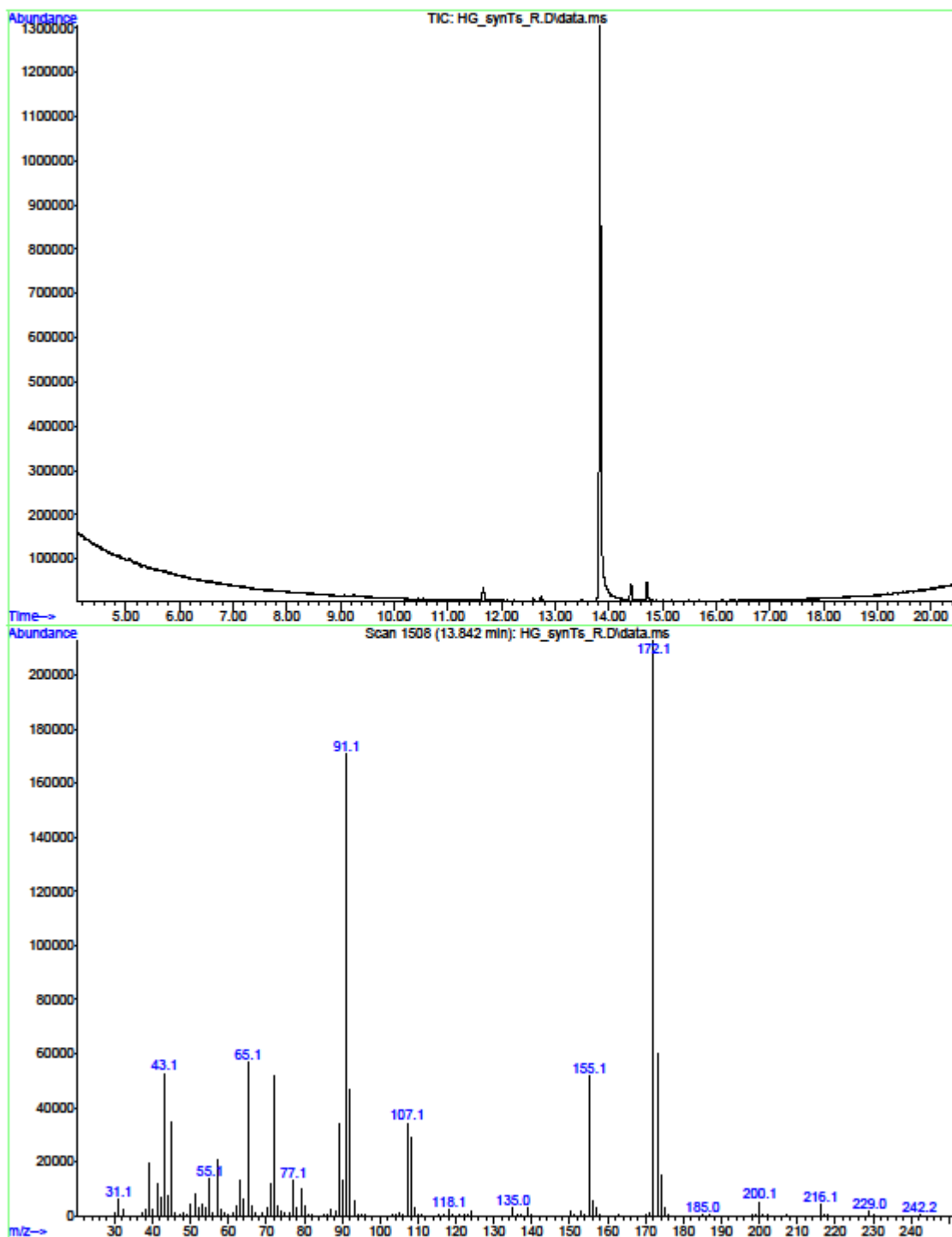


Figure 36 GC-MS spectrum of (*R*)-5

File :C:\msdchem\1\data\Hannes\14-04-01\HG\_SynS\_Tos.D  
Operator : christine  
Acquired : 1 Apr 2014 18:01 using AcqMethod ACHIRAL-MSD.M  
Instrument : 5975  
Sample Name: HG SynS Tos  
Misc Info :  
Vial Number: 1

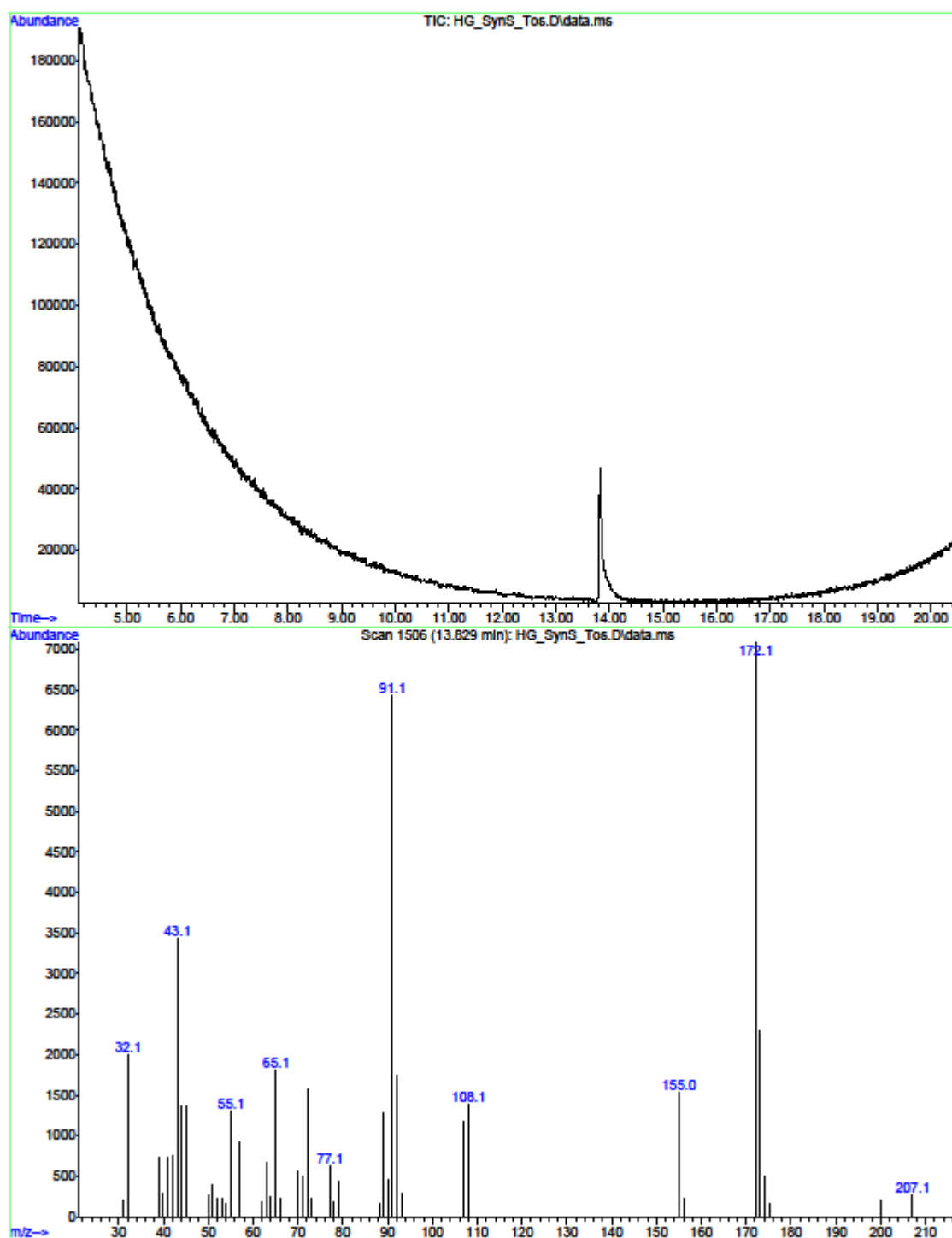


Figure 37 GC-MS spectrum of (S)-5

File :C:\msdchem\1\data\Hannes\14-05-20\HG\_tri-S\_24h.D  
Operator : Hannes  
Acquired : 20 May 2014 9:37 using AcqMethod ACHIRAL-MSD.M  
Instrument : 5975  
Sample Name: HG tri-S 24h  
Misc Info :  
Vial Number: 46

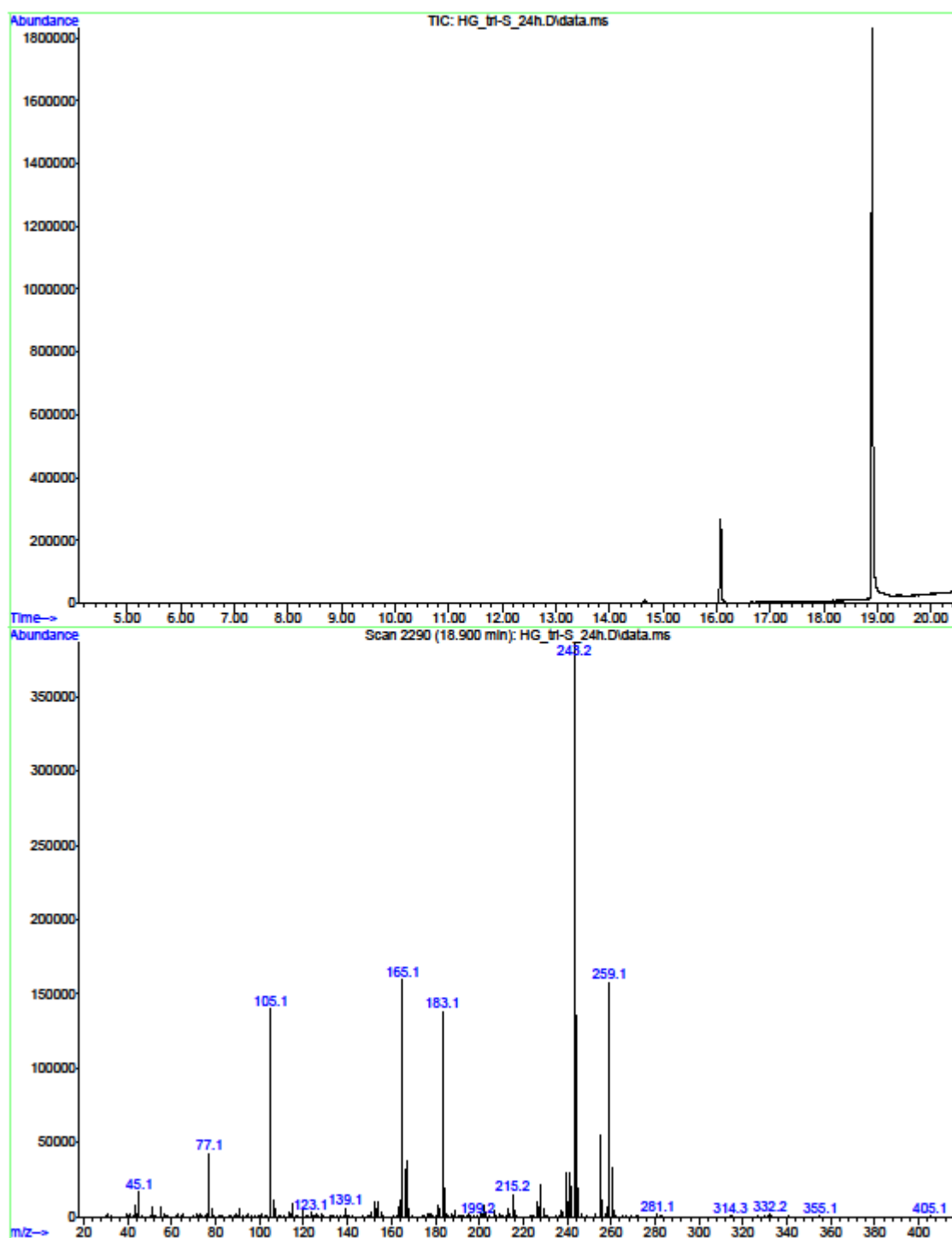


Figure 38 GC-MS spectrum of (S)-6

File : C:\msdchem\1\data\Hannes\14-05-06\HG\_3\_5h.D  
Operator : ninaS  
Acquired : 6 May 2014 17:39 using AcqMethod ACHIRAL-MSD.M  
Instrument : 5975  
Sample Name: HG 3 5h  
Misc Info :  
Vial Number: 43

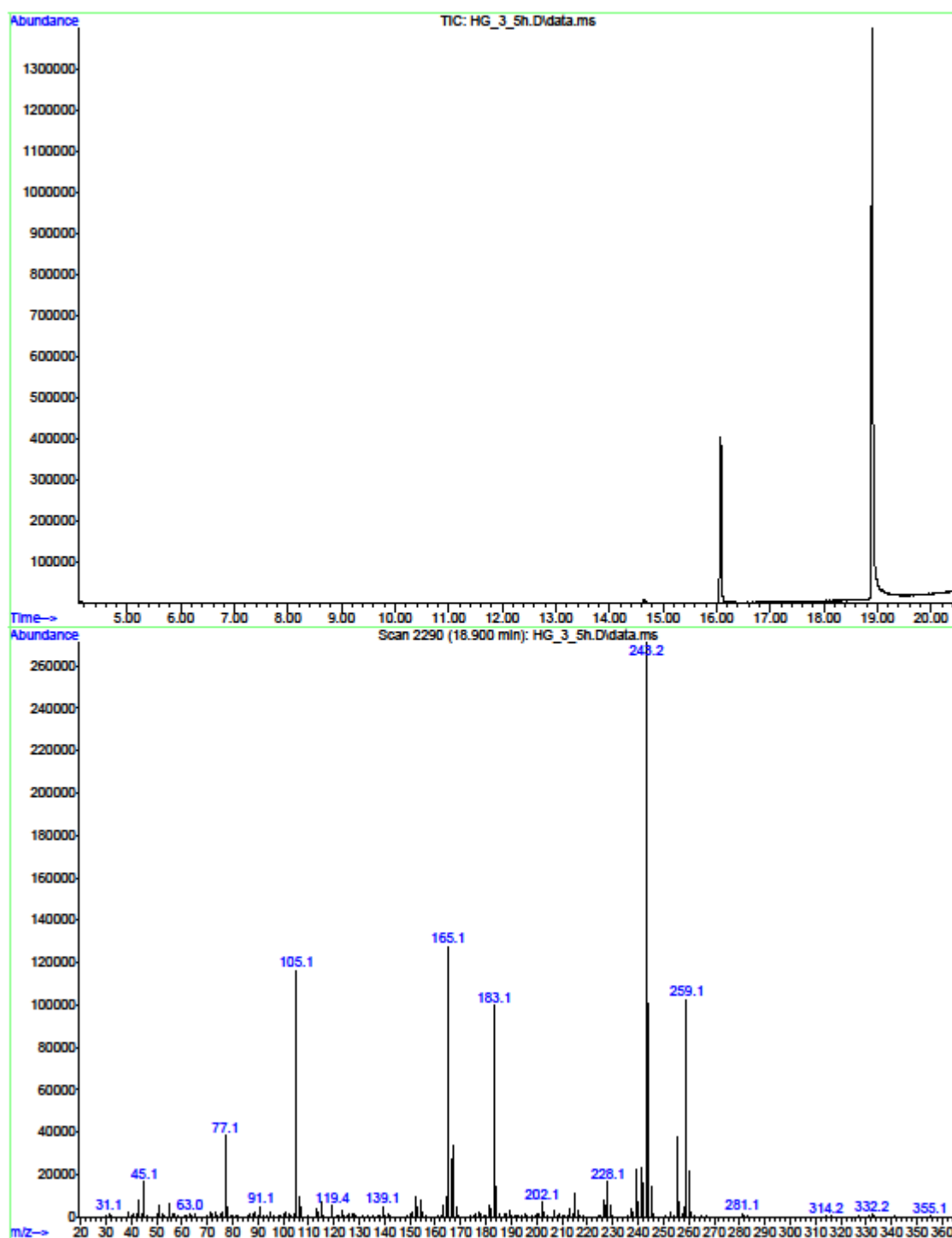


Figure 39 GC-MS spectrum of (*R*)-6

File :C:\msdchem\1\data\Hannes\14-05-22\HG\_Fr5.D  
Operator : nIKI  
Acquired : 22 May 2014 18:35 using AcqMethod ACHIRAL-MSD.M  
Instrument : 5975  
Sample Name: HG Fr5  
Misc Info :  
Vial Number: 39

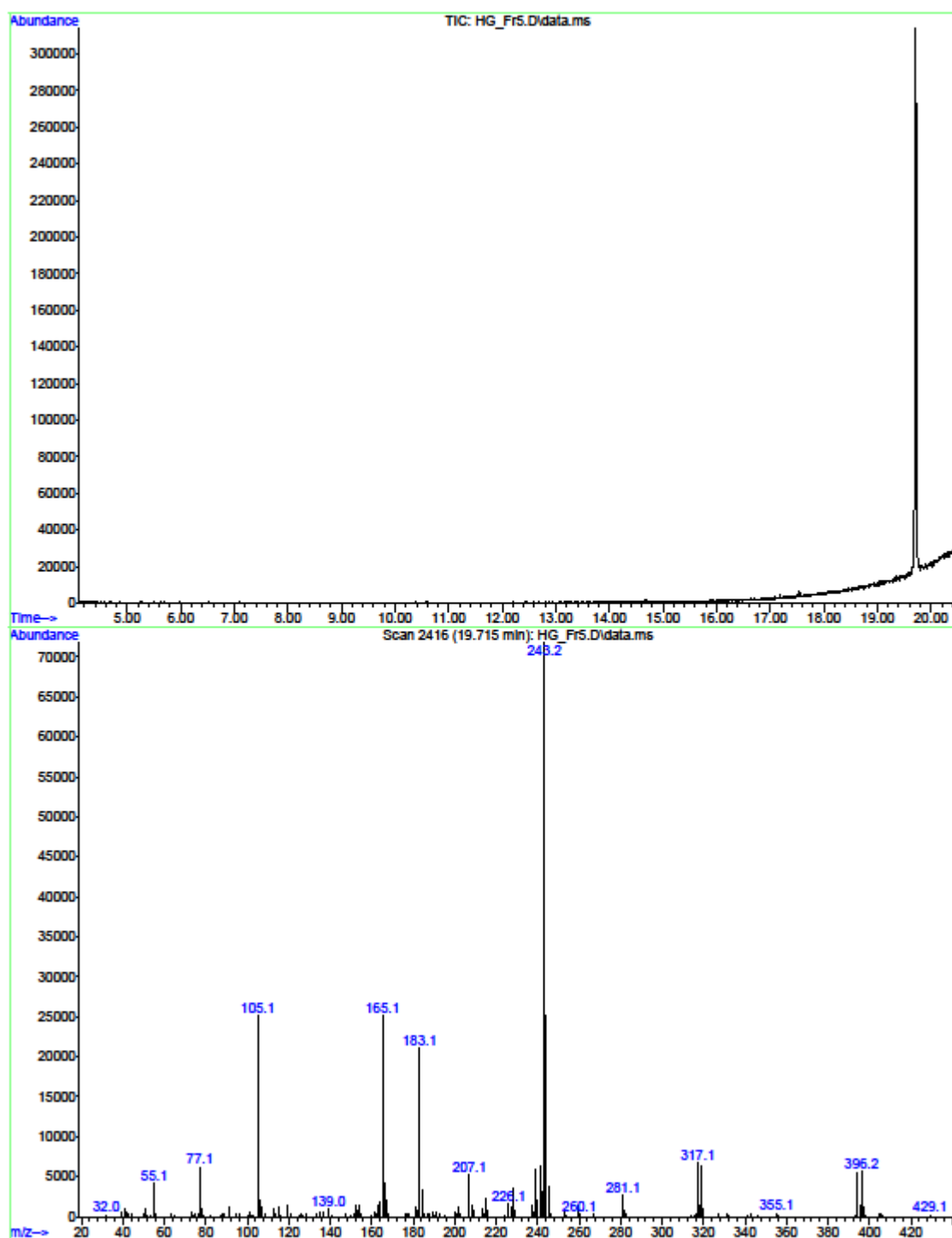


Figure 40 GC-MS spectrum of (R)-7

File : C:\msdchem\1\data\Hannes\14-05-20\HG\_apple.D  
Operator : Hannes  
Acquired : 20 May 2014 15:13 using AcqMethod ACHIRAL-MSD.M  
Instrument : 5975  
Sample Name: HG apple  
Misc Info :  
Vial Number: 51

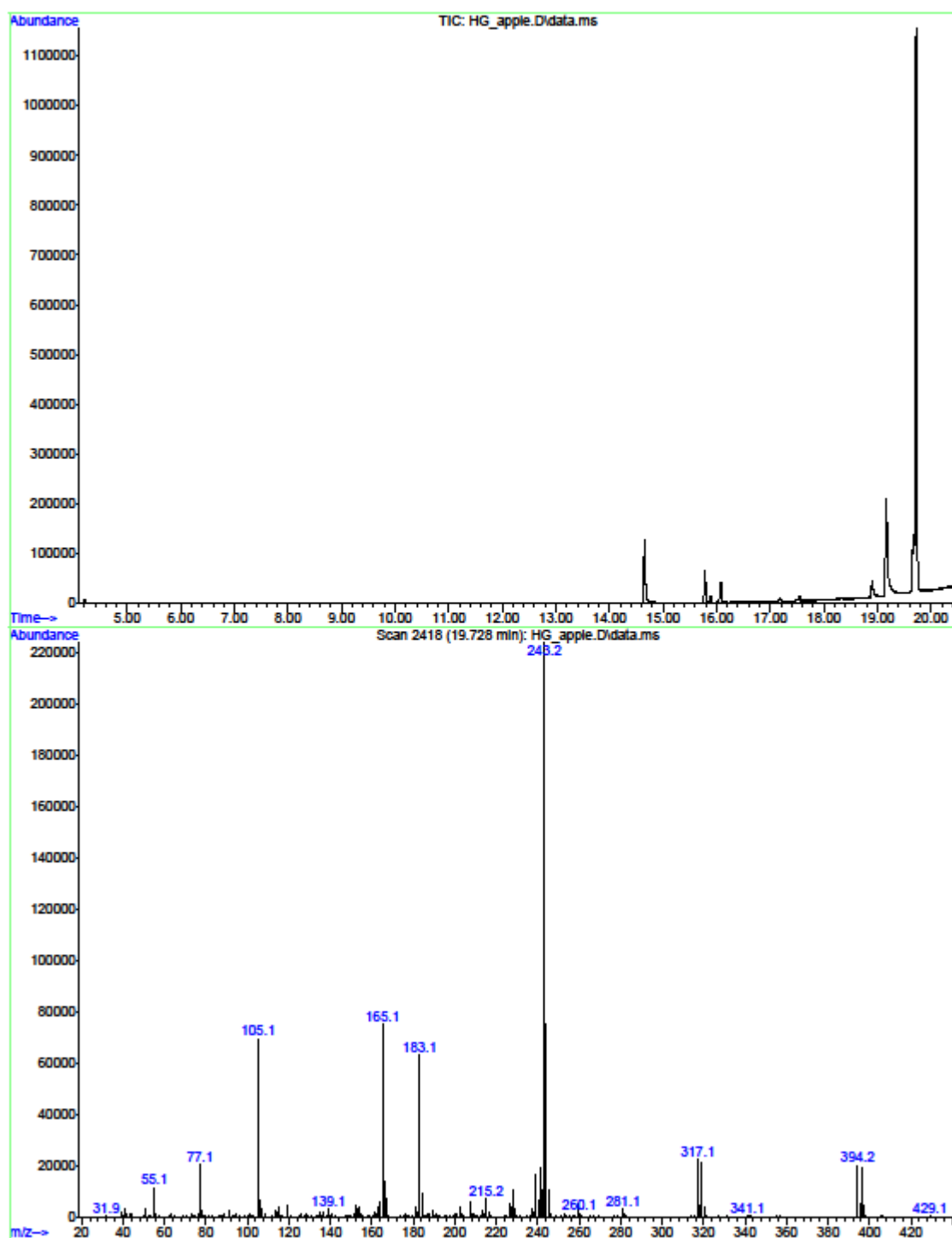


Figure 41 GC-MS spectrum of (R)-7